

Thermal correction to the Casimir force, radiative heat transfer, and an experiment

V. B. Bezerra¹, G. Bimonte^{2,3}, G. L. Klimchitskaya^{4,a}, V. M. Mostepanenko^{4,b}, and C. Romero¹

¹ Department of Physics, Federal University of Paraíba, C.P.5008, CEP 58059–970, João Pessoa, Pb-Brazil

² Dipartimento di Scienze Fisiche, Università di Napoli Federico II, Complesso Universitario MSA, Via Cintia I—80126 Napoli, Italy

³ INFN, Sezione di Napoli, Napoli, Italy

⁴ Center of Theoretical Studies and Institute for Theoretical Physics, Leipzig University, D-04009, Leipzig, Germany

Received: date / Revised version: date

Abstract. The low-temperature asymptotic expressions for the Casimir interaction between two real metals described by Leontovich surface impedance are obtained in the framework of thermal quantum field theory. It is shown that the Casimir entropy computed using the impedance of infrared optics vanishes in the limit of zero temperature. By contrast, the Casimir entropy computed using the impedance of the Drude model attains at zero temperature a positive value which depends on the parameters of a system, i.e., the Nernst heat theorem is violated. Thus, the impedance of infrared optics withstands the thermodynamic test, whereas the impedance of the Drude model does not. We also perform a phenomenological analysis of the thermal Casimir force and of the radiative heat transfer through a vacuum gap between real metal plates. The characterization of a metal by means of the Leontovich impedance of the Drude model is shown to be inconsistent with experiment at separations of a few hundred nanometers. A modification of the impedance of infrared optics is suggested taking into account relaxation processes. The power of radiative heat transfer predicted from this impedance is several times less than previous predictions due to different contributions from the transverse electric evanescent waves. The physical meaning of low frequencies in the Lifshitz formula is discussed. It is concluded that new measurements of radiative heat transfer are required to find out the adequate description of a metal in the theory of electromagnetic fluctuations.

1 Introduction

During the last few years, complicated problems connected with the concept of quantum fluctuations generated much interest among specialists in gravitation and cosmology, dispersion forces, Bose-Einstein condensation, nanotechnology, radiative heat transfer and related subjects. Van der Waals and Casimir forces, which are different kinds of dispersion forces, arise from zero-point oscillations of the electromagnetic field and thermal photons. They act between closely spaced macrobodies, between a microparticle and a macrobody or between two microparticles. The theory of dispersion forces is based on quantum statistical physics. For real bodies at temperature T described by a dielectric permittivity depending only on frequency, the van der Waals and Casimir forces acting between them are calculated in the framework of Lifshitz theory [1,2,3]. Originally Lifshitz theory was developed using the concept

of an oscillating electromagnetic field and the fluctuation-dissipation theorem. Later the main equations of this theory, including the famous Lifshitz formula, were rederived in different formalisms [4,5,6,7] and in particular on the basis of thermal quantum field theory in the Matsubara formulation [8]. The Lifshitz theory was recently used for the interpretation of many experiments on the measurement of the Casimir force [9,10,11,12,13,14,15,16,17,18,19,20,21,22,23,24], in the application of the Casimir and van der Waals forces in nanotechnology [25,26,27,28,29], in Bose-Einstein condensation [30,31] and also for the description of radiative heat transfer between two bodies at different temperatures through a vacuum gap [32,33].

The application of Lifshitz theory to real metallic bodies at nonzero temperature has led to controversial results, depending on the used model of dielectric permittivity. If the boundary bodies are described by the free electron plasma model the ensuing thermal correction to the Casimir force [34,35] is in qualitative agreement with that obtained for ideal metals on the basis of thermal quantum field theory in Matsubara formulation [8,36]. If, however, metal boundaries are described by the Drude model which takes relaxation into account, the thermal correction at

^a On leave from North-West Technical University, Millionnaya St. 5, St.Petersburg, 191065, Russia

^b On leave from Noncommercial Partnership “Scientific Instruments”, Tverskaya St. 11, Moscow, 103905, Russia

short separations is many hundred times larger than for ideal metals and two times smaller than the latter at large separations [37,38]. In the case of perfect crystal lattices with no impurities, the entropy of a fluctuating field (i.e., the Casimir entropy) calculated using the Drude model takes a negative value when the temperature vanishes, i.e., the Nernst heat theorem is violated [39,40]. In [41, 42] it was argued that for real metals with impurities this violation does not occur, but in the case of perfect crystal lattices the problem remains unsolved. If the dielectric permittivity of the plasma model is chosen the Nernst heat theorem is satisfied [39,40]. Importantly, the application of the Drude dielectric function was found to be inconsistent with experiment [16,17,18,19,20]. On the contrary, the plasma model approach is consistent with experimental data [43].

Interestingly, similar problem arises in the theory of the thermal Casimir force acting between dielectrics. If the static dielectric permittivity of dielectric materials is supposed to be finite, Lifshitz theory is found [44,45] to be in agreement with thermodynamics. If, however, the dc conductivity of dielectric materials is taken into account, the Nernst heat theorem for the entropy of a fluctuating field is violated [44,45]. The same is true in the metal-dielectric configuration [46] depending on the finiteness of the static permittivity of a dielectric plate [47,48]. Thus, thermodynamics provides a test for the validity of various models of material properties: only the thermodynamically-consistent models should be used. In this connection it is notable that just the Drude model of a metal, which was shown to imply a violation of the Nernst heat theorem for the Casimir entropy, was found to be in contradiction with experiments (controversial opinions on this subject can be found in [49,50]).

As an alternative to the dielectric model, the optical properties of a metal surface can be characterized in terms of the Leontovich surface impedance, together with the corresponding boundary conditions [51]. In the framework of the Lifshitz theory it was employed in [52] at zero temperature and in [53,54] at nonzero temperature. It should be kept in mind that both models of real metals, the one based on the frequency-dependent dielectric permittivity as well as the one using Leontovich impedance, are approximations, each having its own range of validity. The concept of a frequency-dependent permittivity is inapplicable in the frequency region of the anomalous skin effect, where spatial dispersion contributes critically. Physically this is explained by the fact that for these frequencies the penetration depth of the electromagnetic field inside a metal becomes of the same order as the mean free path of conduction electrons and remains much less than the distance traveled by an electron during the period of the field. As a result, the spatial non-uniformity of the field renders impossible a macroscopic description in terms of a dielectric permittivity depending only on the frequency [51]. On the other hand, impedance boundary conditions retain their validity at the frequencies of the anomalous skin effect because the field inside a metal near the surface

can be considered as a plane wave propagating perpendicular to the surface.

However, Leontovich impedance, though applicable to the description of the anomalous skin effect, cannot be used at short separations where its magnitude is not much less than unity. The physical reason for this is that with decreasing separations the relevant characteristic frequencies enter the optical region, where the field inside a metal cannot be considered anymore as propagating perpendicularly to the metal surface. In this frequency region the concept of dielectric permittivity depending only on the frequency is satisfactory (because the distance traveled by an electron during the period of the field is much less than the penetration depth). However, the magnitude of the dielectric permittivity is not large enough, and, as a consequence, the angle of refraction depends on the angle of incidence. Thus, the impedance boundary condition does not apply.

The explicit analytic forms of the impedance function are available in the asymptotic regions of the normal and anomalous skin effect and in infrared optics. As was noticed without a detailed proof in [54], the Casimir entropy calculated using the impedance of infrared optics vanishes when the temperature goes to zero, i.e., the Nernst heat theorem is satisfied. The same is proved in [55] for the Casimir entropy calculated with the impedance of the anomalous skin effect. We stress that at large separations the impedance approach leads to magnitudes of the thermal Casimir force in qualitative agreement with the case of ideal metals.

A critical problem of the impedance approach is the choice of the functional dependence of the impedance function on the frequency. In [54] it was argued that the impedance function valid in the region around the characteristic frequency should be extrapolated to lower frequencies, all the way to the zero Matsubara frequency. In [56] quantitative arguments were adduced in favor of the statement that the use of different impedance functions within different frequency regions in accordance with their applicability conditions would be thermodynamically inconsistent. In the first part of this paper we apply the thermodynamic test to the impedance function of [33] which provides a smooth analytic interpolation between the impedances of the normal skin effect and infrared optics. The substitution of the interpolated impedance [33] in the Lifshitz formula presents an explicit example of the situation where different impedances are used at Matsubara frequencies belonging to different frequency regions. We present a rigorous analytic proof that the entropy of a fluctuating field in this situation goes to a positive value when the temperature vanishes. In other words, the Lifshitz formula combined with the interpolated impedance is thermodynamically inconsistent.

The problem of the thermal correction to the Casimir force was further discussed in [57,58,59] where the impedance of the normal skin effect was used in the computations. In this approach at a separation of $1\ \mu\text{m}$ the thermal correction was found to be about 30 times larger than for ideal metal plates. This was explained by the dominant

contribution of the transverse electric evanescent waves of rather low frequencies. The same impedance function was applied [33] to compute the radiative heat transfer through a vacuum gap between two metal surfaces at different temperatures. This problem was considered previously in [60,61] (and recently in [32]) using the formalism of dielectric permittivity. As proposed in [33], the problems of the thermal Casimir force and the radiative heat transfer through a vacuum gap are closely related and their simultaneous investigation can be very fruitful and elucidating.

In the second part of this paper we consider both the thermal correction to the Casimir force and the power of radiative heat transfer using different impedance functions and compare the results with those obtained previously using the formalism of dielectric permittivity and with experiment. We try to address, from a purely phenomenological point of view, the radiative heat transfer through a vacuum gap in connection with the problem of thermal Casimir force between real metals. The aim of our work on this subject is to come up with a phenomenological model for a real metal at room temperature, that takes dissipation into account, and is at the same time consistent with available experimental facts. In view of the existing controversies among theoreticians about the correct way to do this, it is our view that finding a reasonable empirical model would be a valuable guide for further theoretical studies. We perform computations in the framework of two different formulations of Lifshitz theory along the real and the imaginary frequency axis. This permits to specify the comparative role of the travelling and evanescent waves in the physical phenomena under consideration and to determine the application range of different approximations. It is shown that use of the impedance of the normal skin effect results in enormously large thermal corrections to the Casimir force at separations of about 200–300 nm which are inconsistent with already performed experiments. As an alternative, a phenomenological generalized impedance of infrared optics is constructed taking into account relaxation processes specific for this frequency region which are not connected with the electron-phonon interactions. The thermal correction to the Casimir force computed with the generalized impedance function is shown to be qualitatively the same as is known for ideal metals from thermal quantum field theory in Matsubara formulation. It is consistent with all available experimental data. The suggested impedance function is applied to calculate the power of radiative heat transfer between Au plates at different temperatures. At short separations between the plates the obtained power of heat transfer per unit area is several times less than the one predicted previously in literature using the dielectric function or the impedance characteristic for the region of the normal skin effect. Thus we find that, depending on the chosen model of the metal, one obtains largely different predictions for both the thermal Casimir force and the power of radiative heat transfer. This result underlines the crucial role of new experiments on the precision measurements of the Casimir force and the power of radiative heat transfer.

The paper is organized as follows. In Sec. 2 we present two equivalent forms of Lifshitz formula, which involve evaluating the reflection coefficients for imaginary and real frequencies, respectively. In Sec. 3 we give the explicit expressions of the reflection coefficients in terms of a frequency dependent dielectric permittivity and in terms of Leontovich surface impedance. In Sec. 4 we demonstrate that Lifshitz formula combined with the impedance function of the infrared optics is thermodynamically consistent. In Sec. 5 we prove that the substitution of the interpolated impedance into the Lifshitz formula results in a violation of the Nernst heat theorem. Sec. 6 is devoted to the computation of the thermal correction to the Casimir force using different impedance functions. The results are compared with the case of plates made of ideal metal and with experiment. In Sec. 7 the general expression for the power per unit area of radiative heat transfer in terms of the surface impedance is presented. Sec. 8 contains the computation results for radiative heat transfer with different impedances and dielectric permittivities including the new prediction to be tested experimentally. In Sec. 9 the reader will find our conclusions and discussion.

2 Lifshitz formula along the imaginary and real frequency axis

In this section we consider two thick dissimilar plane parallel plates (semispaces) in thermal equilibrium at equal temperature T , separated by an empty gap of width a . Let the z axis be perpendicular to the plates. The Lifshitz formula [1] represents the van der Waals and Casimir free energy and force per unit area (i.e., the pressure), acting between the plates marked by the indices (1) and (2), in terms of the reflection coefficients $r_{\text{TM}}^{(1,2)}(\omega, k_{\perp})$ and $r_{\text{TE}}^{(1,2)}(\omega, k_{\perp})$ for two independent polarizations of electromagnetic field (ω is the frequency and k_{\perp} is the magnitude of the projection of the wave vector in the plane of the plates). The transverse magnetic polarization (TM) means that the magnetic field is perpendicular to the plane formed by \mathbf{k}_{\perp} and the z axis, while for the transverse electric polarization (TE) the electric field is perpendicular to this plane. As was mentioned in the Introduction, in the literature there are many different derivations of the Lifshitz formula in the framework of quantum statistical physics, thermal quantum field theory in Matsubara formulation and scattering theory (see, e.g., [4, 5, 6, 7, 8]). The final results of all derivations are represented in one of two different forms, as a summation over the Matsubara frequencies along the imaginary frequency axis or, alternatively, as an integral over real frequencies. We begin with the more often used representation in terms of imaginary frequencies, where the Casimir free energy and pressure are given by

$$\mathcal{F}(a, T) = \frac{k_B T}{2\pi} \sum_{l=0}^{\infty} \left(1 - \frac{1}{2} \delta_{l0}\right) \int_0^{\infty} k_{\perp} dk_{\perp} \quad (1)$$

$$\times \sum_{\alpha=\text{TE, TM}} \ln \left[1 - r_{\alpha}^{(1)}(i\xi_l, k_{\perp}) r_{\alpha}^{(2)}(i\xi_l, k_{\perp}) e^{-2a q_l}\right],$$

$$P(a, T) = -\frac{k_B T}{\pi} \sum_{l=0}^{\infty} \left(1 - \frac{1}{2} \delta_{l0}\right) \int_0^{\infty} k_{\perp} dk_{\perp} q_l \quad (2)$$

$$\times \sum_{\alpha=\text{TE, TM}} \left[\frac{e^{2aq_l}}{r_{\alpha}^{(1)}(i\xi_l, k_{\perp}) r_{\alpha}^{(2)}(i\xi_l, k_{\perp})} - 1 \right]^{-1}.$$

Here $\xi_l = 2\pi k_B T l / \hbar$ are the Matsubara frequencies, k_B is Boltzmann constant, l is a non-negative integer and

$$q(\omega, k_{\perp}) = \sqrt{k_{\perp}^2 - \frac{\omega^2}{c^2}}, \quad (3)$$

$$q_l \equiv q(i\xi_l, k_{\perp}) = \sqrt{k_{\perp}^2 + \frac{\xi_l^2}{c^2}}.$$

The explicit form of the reflection coefficients $r_{\alpha}^{(1,2)}$ is discussed in the next section. Representation (2) is convenient in numerical computations due to fast convergence of both the sum and the integrals.

Using the Abel-Plana formula [8, 62]

$$\sum_{l=0}^{\infty} \left(1 - \frac{1}{2} \delta_{l0}\right) F(l) = \int_0^{\infty} F(t) dt \quad (4)$$

$$+ i \int_0^{\infty} dt \frac{F(it) - F(-it)}{e^{2\pi t} - 1},$$

where $F(z)$ is an analytic function in the right half-plane, Eqs. (1) and (2) can be identically rearranged in the form

$$\mathcal{F}(a, T) = E(a) + \Delta\mathcal{F}(a, T),$$

$$P(a, T) = P_0(a) + \Delta P(a, T). \quad (5)$$

Here $E(a)$ is given by

$$E(a) = \frac{\hbar}{4\pi^2} \int_0^{\infty} d\xi \int_0^{\infty} k_{\perp} dk_{\perp} \quad (6)$$

$$\times \sum_{\alpha=\text{TE, TM}} \ln \left[1 - r_{\alpha}^{(1)}(i\xi, k_{\perp}) r_{\alpha}^{(2)}(i\xi, k_{\perp}) e^{-2aq} \right]$$

with $q \equiv q(i\xi, k_{\perp})$ defined in Eqs. (3). The other contribution on the right-hand side of the first equality in Eq. (5) can be represented in the form

$$\Delta\mathcal{F}(a, T) = \frac{ik_B T}{2\pi} \int_0^{\infty} dt \frac{\Phi(i\xi_1 t) - \Phi(-i\xi_1 t)}{e^{2\pi t} - 1}, \quad (7)$$

where $\Phi(x) \equiv \Phi_{\text{TM}}(x) + \Phi_{\text{TE}}(x)$ and

$$\Phi_{\text{TM, TE}}(x) = \int_0^{\infty} k_{\perp} dk_{\perp} \quad (8)$$

$$\times \ln \left[1 - r_{\text{TM, TE}}^{(1)}(ix, k_{\perp}) r_{\text{TM, TE}}^{(2)}(ix, k_{\perp}) e^{2a\sqrt{k_{\perp}^2 + \frac{x^2}{c^2}}} \right].$$

In a similar way, the quantities $P_0(a)$ and $\Delta P(a, T)$ in the second equality in Eq. (5) are equal to

$$P_0(a) = -\frac{\hbar}{2\pi^2} \int_0^{\infty} d\xi \int_0^{\infty} k_{\perp} dk_{\perp} q$$

$$\times \sum_{\alpha=\text{TE, TM}} \left[\frac{e^{2aq}}{r_{\alpha}^{(1)}(i\xi, k_{\perp}) r_{\alpha}^{(2)}(i\xi, k_{\perp})} - 1 \right]^{-1}, \quad (9)$$

$$\Delta P(a, T) = -\frac{ik_B T}{\pi} \int_0^{\infty} dt \frac{F(i\xi_1 t) - F(-i\xi_1 t)}{e^{2\pi t} - 1}, \quad (10)$$

where $F(x) \equiv F_{\text{TM}}(x) + F_{\text{TE}}(x)$ and

$$F_{\text{TM, TE}}(x) = \int_0^{\infty} k_{\perp} dk_{\perp} q \sqrt{k_{\perp}^2 + \frac{x^2}{c^2}} \quad (11)$$

$$\times \left[\frac{e^{2a\sqrt{k_{\perp}^2 + \frac{x^2}{c^2}}}}{r_{\text{TM, TE}}^{(1)}(ix, k_{\perp}) r_{\text{TM, TE}}^{(2)}(ix, k_{\perp})} - 1 \right]^{-1}.$$

Note that the quantities $E(a)$ and $P_0(a)$ in Eqs. (6) and (9) are often called in literature the Casimir energy and pressure at zero temperature, and $\Delta\mathcal{F}(a, T)$ and $\Delta P(a, T)$ in Eqs. (7) and (10) are referred to as the thermal corrections to them. This terminology is, however, correct only for plate materials with temperature independent properties. In this case the Casimir free energy and pressure depend on temperature only through the Matsubara frequencies and the thermal corrections defined as $\mathcal{F}(a, T) - \mathcal{F}(a, 0)$ and $P(a, T) - P(a, 0)$ coincide with $\Delta\mathcal{F}(a, T)$ and $\Delta P(a, T)$ in Eqs. (7) and (10). If, however, the properties of a medium (for instance, the dielectric permittivity) depend on the temperature, then the thermal corrections $\mathcal{F}(a, T) - \mathcal{F}(a, 0)$ and $P(a, T) - P(a, 0)$ do not coincide with $\Delta\mathcal{F}(a, T)$ and $\Delta P(a, T)$. Even in this case Eq. (5) can be used to compute the total Casimir free energy and pressure. In so doing, the quantities $E(a)$ and $P_0(a)$ in Eqs. (6) and (9) can be interpreted as the contributions to the total Casimir free energy and pressure due to zero-point oscillations [they may depend on the temperature as a parameter, i.e., in fact $E(a) = E(a, T)$ and $P_0(a) = P_0(a, T)$] and the quantities $\Delta\mathcal{F}(a, T)$ and $\Delta P(a, T)$ in Eqs. (7) and (10) as the contributions from thermal photons.

It is useful to express the Casimir free energy and pressure as the integrals over *real* frequencies ω :

$$\mathcal{F}(a, T) = \frac{\hbar}{4\pi^2} \int_0^{\infty} d\omega \int_0^{\infty} dk_{\perp} k_{\perp} \coth\left(\frac{\hbar\omega}{2k_B T}\right) \quad (12)$$

$$\times \text{Im} \sum_{\alpha=\text{TE, TM}} \ln \left[1 - r_{\alpha}^{(1)}(\omega, k_{\perp}) r_{\alpha}^{(2)}(\omega, k_{\perp}) e^{2ik_z a} \right],$$

$$P(a, T) = -\frac{\hbar}{2\pi^2} \int_0^{\infty} d\omega \int_0^{\infty} dk_{\perp} k_{\perp} \coth\left(\frac{\hbar\omega}{2k_B T}\right) \quad (13)$$

$$\times \text{Re} \left\{ k_z \sum_{\alpha=\text{TE, TM}} \left[1 - \frac{e^{-2ik_z a}}{r_{\alpha}^{(1)}(\omega, k_{\perp}) r_{\alpha}^{(2)}(\omega, k_{\perp})} \right]^{-1} \right\},$$

where

$$k_z(\omega, k_{\perp}) \equiv \sqrt{\omega^2/c^2 - k_{\perp}^2} = iq(\omega, k_{\perp}). \quad (14)$$

We note that real values of k_z correspond to propagating waves (PW), while imaginary values of k_z describe evanescent waves (EW). Upon using the identity

$$\coth(x/2) = 1 + \frac{2}{\exp(x) - 1}, \quad (15)$$

we see that the formula for the Casimir pressure can be expressed as the sum of two terms, like in Eq. (5)

$$P(a, T) = P_0(a, T) + \Delta P(a, T), \quad (16)$$

where

$$P_0(a, T) = -\frac{\hbar}{2\pi^2} \int_0^\infty d\omega \int_0^\infty dk_\perp k_\perp \quad (17)$$

$$\times \operatorname{Re} \left\{ k_z \sum_{\alpha=\text{TE, TM}} \left[1 - \frac{e^{-2ik_z a}}{r_\alpha^{(1)}(\omega, k_\perp) r_\alpha^{(2)}(\omega, k_\perp)} \right]^{-1} \right\},$$

and

$$\Delta P(a, T) = -\frac{\hbar}{\pi^2} \int_0^\infty d\omega \int_0^\infty dk_\perp k_\perp \frac{1}{\exp\left(\frac{\hbar\omega}{k_B T}\right) - 1}$$

$$\times \operatorname{Re} \left\{ k_z \sum_{\alpha=\text{TE, TM}} \left[1 - \frac{e^{-2ik_z a}}{r_\alpha^{(1)}(\omega, k_\perp) r_\alpha^{(2)}(\omega, k_\perp)} \right]^{-1} \right\}. \quad (18)$$

Similar representations can be easily obtained for $E(a, T)$ and $\Delta \mathcal{F}(a, T)$. As was already noted above, $P_0(a, T)$ physically represents the contribution to the pressure from zero-point fluctuations of the electromagnetic field, and in general it depends on the temperature, because the permittivities or surface impedances of the plates are temperature-dependent. As for $\Delta P(a, T)$, it represents the contribution from thermally excited electromagnetic fields, and it vanishes for $T = 0$. For this reason, in what follows we shall conventionally refer to $\Delta P(a, T)$ as to the thermal correction to the Casimir pressure. We further consider the decomposition

$$\Delta P(a, T) = \Delta P_{\text{PW}}(a, T) + \Delta P_{\text{EW}}(a, T), \quad (19)$$

where $\Delta P_{\text{PW}}(a, T)$ and $\Delta P_{\text{EW}}(a, T)$ represent the contributions from PW and EW, respectively. It is easily seen from Eq. (18) that $\Delta P_{\text{PW}}(a, T)$ can be written as:

$$\Delta P_{\text{PW}}(a, T) = -\frac{\hbar}{\pi^2} \int_0^\infty d\omega \frac{1}{\exp\left(\frac{\hbar\omega}{k_B T}\right) - 1} \int_0^{\omega/c} dk_z k_z^2$$

$$\times \sum_{\alpha=\text{TE, TM}} \operatorname{Re} \left[1 - \frac{e^{-2ik_z a}}{r_\alpha^{(1)}(\omega, k_\perp) r_\alpha^{(2)}(\omega, k_\perp)} \right]^{-1}. \quad (20)$$

For EW it holds $k_\perp > \omega/c$ and $\operatorname{Im}(k_z) = q$. As a result $\Delta P_{\text{EW}}(a, T)$ takes the form

$$\Delta P_{\text{EW}}(a, T) = \frac{\hbar}{\pi^2} \int_0^\infty d\omega \frac{1}{\exp\left(\frac{\hbar\omega}{k_B T}\right) - 1} \int_0^\infty dq q^2$$

$$\times \sum_{\alpha=\text{TE, TM}} \operatorname{Im} \left[1 - \frac{e^{2qa}}{r_\alpha^{(1)}(\omega, k_\perp) r_\alpha^{(2)}(\omega, k_\perp)} \right]^{-1}. \quad (21)$$

It should be noted that $\Delta P_{\text{EW}}(a, T)$ vanishes in the case of ideal metals, because for $r_\alpha^{(1)} r_\alpha^{(2)} = 1$ the quantity between square brackets in the above equation is real. In fact, more generally $\Delta P_{\text{EW}}(a, T)$ vanishes whenever the product of the reflection coefficients $r_\alpha^{(i)}$ is real and less or equal to unity, because then the quantity between the square brackets in Eq. (21) is real and has no zeroes. This is the case for example for TE EW, if the metal plates are described by the plasma model (see below).

3 Reflection coefficients in terms of the dielectric permittivity and the surface impedance

In Lifshitz theory the material media are described by dielectric permittivities that depend only on frequency [1, 2, 3]. The description of the dielectric properties of a medium by $\varepsilon(\omega)$ takes full account of temporal dispersion but neglects possible contributions to the van der Waals and Casimir force from spatial dispersion. In the formalism of the imaginary frequency axis [see Eqs. (1) and (2)] the reflection coefficients are expressed in terms of the dielectric permittivity as follows:

$$r_{\text{TM}}^{(n)}(i\xi_l, k_\perp) = \frac{\varepsilon^{(n)}(i\xi_l)q_l - k_l^{(n)}}{\varepsilon^{(n)}(i\xi_l)q_l + k_l^{(n)}},$$

$$r_{\text{TE}}^{(n)}(i\xi_l, k_\perp) = \frac{k_l^{(n)} - q_l}{k_l^{(n)} + q_l}, \quad (22)$$

where $n = 1, 2$ for the first and the second plates, respectively, and

$$k^{(n)}(\omega, k_\perp) = \sqrt{k_\perp^2 - \varepsilon^{(n)}(\omega) \frac{\omega^2}{c^2}}, \quad (23)$$

$$k_l^{(n)} \equiv k^{(n)}(i\xi_l, k_\perp) = \sqrt{k_\perp^2 + \varepsilon^{(n)}(i\xi_l) \frac{\xi_l^2}{c^2}}.$$

In the formalism of real frequency axis used in Eqs. (12) and (13) the reflection coefficients are just (22) but calculated at real frequencies

$$r_{\text{TM}}^{(n)}(\omega, k_\perp) = \frac{\varepsilon^{(n)}(\omega)q(\omega, k_\perp) - k^{(n)}(\omega, k_\perp)}{\varepsilon^{(n)}(\omega)q(\omega, k_\perp) + k^{(n)}(\omega, k_\perp)},$$

$$r_{\text{TE}}^{(n)}(\omega, k_\perp) = \frac{k^{(n)}(\omega, k_\perp) - q(\omega, k_\perp)}{k^{(n)}(\omega, k_\perp) + q(\omega, k_\perp)}. \quad (24)$$

The reflection properties of electromagnetic waves on metal surfaces are often described in terms of the Leontovich surface impedance [51]. For isotropic metal surfaces the surface impedance relates the tangential components of electric field and magnetic induction in the same way as in a plane wave propagating in the interior of a metal perpendicular to its surface [51]

$$\mathbf{E}_t = Z(\omega) [\mathbf{B}_t \times \mathbf{n}], \quad (25)$$

Here \mathbf{n} is the unit vector normal to the surface and directed inside the medium. For an ideal metal $Z = 0$. The boundary condition (25) is valid when $|Z| \ll 1$. For good conductors this inequality is satisfied within a wide frequency region. Equation (25) permits to determine the electromagnetic field outside the metal, without considering the propagation of electromagnetic waves in the metal interior. It is close in spirit to the original Casimir approach for ideal metals and to so-called ‘‘nonlocal’’ boundary condition [63] implied by a dielectric permittivity depending only on the frequency. The latter condition is in

fact equivalent to the standard continuity boundary conditions in classical electrodynamics but does not require to consider field propagation inside a metal. Both the standard continuity conditions and the “nonlocal” boundary condition are based on the spatially local relation $\mathbf{D}(\mathbf{x}, \omega) = \varepsilon(\omega)\mathbf{E}(\mathbf{x}, \omega)$ which assumes space homogeneity. Therefore these boundary conditions do not take into account the effects of spatial dispersion. As a consequence, the standard Lifshitz formula is applicable only in the absence of spatial dispersion. An advantage of the surface impedance, as compared with dielectric permittivity, is that it permits [52] to apply the Lifshitz formula in the region of the anomalous skin effect, where the spatial homogeneity is violated and the effects of spatial dispersion should be taken into consideration. In [64] the applicability of the condition (25) in the region of the anomalous skin effect is demonstrated from the solution of kinetic equations. In this frequency region, a metal cannot be characterized by a dielectric permittivity depending only on frequency and, thus, the standard Lifshitz formula is not applicable [65] (the Leontovich impedance, however, cannot be used at short separations between the plates where the condition $|Z| \ll 1$ is violated, see Introduction). In the frequency regions where both quantities $\varepsilon(\omega)$ and $Z(\omega)$ are well defined it holds

$$Z(\omega) = 1/\sqrt{\varepsilon(\omega)}. \quad (26)$$

In optics of metals the reflection coefficients are usually expressed in terms of $Z(\omega)$ rather than $\varepsilon(\omega)$ [51]. In [52] the Leontovich surface impedance was used to express the reflection coefficients in the Lifshitz formula at zero temperature. The thermal Casimir force was presented in terms of the surface impedance in [53]. The derivation of the Lifshitz formula starting from impedance boundary condition (25) is contained in [54]. Importantly, as was shown in [54], the use of the Leontovich impedance leads to different results for the thermal Casimir force between real metals, than are obtained by the use of the Drude dielectric function in [37]. The thermal Casimir force computed within the impedance approach was demonstrated to be in qualitative agreement with the case of ideal metals and in accordance with the fundamentals of thermodynamics and with experiment. (The controversies between different approaches to the thermal Casimir force are discussed in detail in [42, 50, 66, 67]).

Using the Leontovich surface impedance instead of the dielectric permittivity, the reflection coefficients in Eqs. (1) and (2) (in the formalism of the imaginary frequency axis) are given by

$$\begin{aligned} r_{\text{TM}}^{(n)}(i\xi_l, k_\perp) &= \frac{cq_l - Z^{(n)}(i\xi_l)\xi_l}{cq_l + Z^{(n)}(i\xi_l)\xi_l}, \\ r_{\text{TE}}^{(n)}(i\xi_l, k_\perp) &= \frac{\xi_l - cq_l Z^{(n)}(i\xi_l)}{\xi_l + cq_l Z^{(n)}(i\xi_l)}. \end{aligned} \quad (27)$$

In the formalism of real frequency axis, the reflection coefficients expressed in terms of the Leontovich impedance

are

$$\begin{aligned} r_{\text{TM}}^{(n)}(\omega, k_\perp) &= \frac{ck_z(\omega, k_\perp) - Z^{(n)}(\omega)\omega}{ck_z(\omega, k_\perp) + Z^{(n)}(\omega)\omega}, \\ r_{\text{TE}}^{(n)}(\omega, k_\perp) &= \frac{\omega - ck_z(\omega, k_\perp)Z^{(n)}(\omega)}{\omega + ck_z(\omega, k_\perp)Z^{(n)}(\omega)}, \end{aligned} \quad (28)$$

where k_z is defined in Eq. (14). An important problem arising in the case of real metals is the adequate choice of the functions $\varepsilon(\omega)$ and $Z(\omega)$.

The calculation of the surface impedance over the whole frequency axis is based on kinetic theory [64]. Here we are interested in two frequency regions. One of them is the infrared optics defined by the inequalities

$$\frac{v_F}{\omega} \ll \delta_i \ll l(T), \quad \omega \ll \omega_p, \quad (29)$$

where v_F is the Fermi velocity, $l(T)$ is the mean free path of a conduction electron, $\delta_i = c/\omega_p$ is the skin depth and $\omega_p = 2\pi c/\lambda_p$ is the plasma frequency. The other frequency region of our interest is the region of the normal skin effect characterized by the inequalities

$$l(T) \ll \delta_N(\omega, T), \quad l(T) \ll \frac{v_F}{\omega}, \quad (30)$$

where $\delta_N(\omega, T) = c/\sqrt{2\pi\sigma_0(T)\omega}$ and $\sigma_0(T)$ is the static electric conductivity.

In the frequency regions (29) and (30), both the dielectric permittivity and the impedance have definite physical meanings and are connected by Eq. (26). In the region of the infrared optics we have

$$\varepsilon_i(\omega) = 1 - \frac{\omega_p^2}{\omega^2}, \quad Z_i(\omega) = -i \frac{\omega}{\sqrt{\omega_p^2 - \omega^2}}. \quad (31)$$

For the normal skin effect (30) we have

$$\begin{aligned} \varepsilon_N(\omega) \equiv \varepsilon_N(\omega, T) &= i \frac{4\pi\sigma_0(T)}{\omega}, \\ Z_N(\omega) \equiv Z_N(\omega, T) &= (1 - i) \sqrt{\frac{\omega}{8\pi\sigma_0(T)}}. \end{aligned} \quad (32)$$

Let us consider two plates at room temperature $T = 300$ K at the same separation distance of a few hundred nanometers, as in [33]. In this case, the respective characteristic frequency of the Casimir effect $\Omega_c = c/(2a)$ belongs to the region of infrared optics (29). (As an example, at $a = 400$ nm, $\Omega_c = 3.75 \times 10^{14}$ rad/s and for gold $\omega_p \approx 1.37 \times 10^{16}$ rad/s and $v_F \approx 1.78 \times 10^6$ m/s.) In the Lifshitz formulas (1), (2) and (12), (13) the frequencies of order ω_p and higher practically do not contribute to the result. All Matsubara frequencies ξ_l in Eqs. (1) and (2), which contribute to the result essentially, belong to the region of infrared optics (29) with the exception of $\xi_0 = 0$, which belongs to the region of the normal skin effect (30) (recall that $\xi_1 = 2.47 \times 10^{14}$ rad/s). Real frequencies in Eqs. (12) and (13), contributing to the result, also belong

to the region of infrared optics (29) and to the normal skin effect (30).

In [33] the correlation functions of a fluctuating electromagnetic field were expressed in terms of the surface impedance. The developed formalism was applied to derive the Lifshitz formulas (12) and (13) along the real frequency axis and to describe the radiation heat transfer between two semispaces at different temperatures. We consider the impedance function defined by the Drude dielectric function which was used in [33]

$$Z_D(\omega) = \frac{1}{\sqrt{\varepsilon_D(\omega)}}, \quad \varepsilon_D(\omega) = 1 - \frac{\omega_p^2}{\omega[\omega + i\gamma(T)]}. \quad (33)$$

Here $\gamma(T)$ is the relaxation parameter connected with the above used parameters by the equation [68]

$$\omega_p^2 = 4\pi\gamma(T)\sigma_0(T) = \frac{4\pi\sigma_0(T)}{\tau(T)}, \quad (34)$$

where $\tau = 1/\gamma$ is the relaxation time. In the region of infrared optics we have $\gamma(T) \ll \omega$. As a result, Z_D and ε_D in Eq. (33) coincide with Z_i and ε_i in Eq. (31), respectively. At small frequencies, on the contrary, one can neglect ω , as compared to γ , and from Eq. (34) Z_D and ε_D in Eq. (33) coincide with Z_n and ε_n in Eq. (32) describing the frequency region of the normal skin effect. Therefore, Eq. (33) provides an expression of the impedance which is valid in both frequency regions of the normal skin effect and infrared optics, and it represents a smooth analytic interpolation between the two regions.

Below we demonstrate that the impedance of infrared optics, Z_i , extrapolated to all lower frequencies, including zero frequency, leads to zero entropy of a fluctuating field at $T = 0$ (Sec. 4). At the same time, the entropy of a fluctuating field calculated using the impedance of the Drude model in Eq. (33) approaches a nonzero positive value when the temperature vanishes (Sec. 5), hence violating thermodynamics.

4 Thermodynamic test for the surface impedance of infrared optics

We consider the free energy of a fluctuating field given by Eqs. (1) and (12) with reflection coefficients (27), (28) and the impedance function (31). Our aim is to find the asymptotic behavior of the free energy and entropy of a fluctuating field at low temperatures at separation distances between two similar plates of a few hundred nanometers, so that the characteristic frequency Ω_c belongs to the region of infrared optics. The perturbation expansions in powers of the small parameter $\kappa \equiv 4\pi k_B a T / (\hbar c)$ can be conveniently carried out by using the dimensionless variables

$$\zeta_l \equiv \frac{\xi_l}{\Omega_c} = \frac{2a\xi_l}{c} = \kappa l, \quad y = 2aq_l. \quad (35)$$

In terms of these variables the free energy of the fluctuating field, Eq. (1), takes the form

$$\mathcal{F}(a, T) = \frac{\hbar c \kappa}{32\pi^2 a^3} \sum_{l=0}^{\infty} \left(1 - \frac{1}{2}\delta_{0l}\right) \int_{\zeta_l}^{\infty} y dy \quad (36)$$

$$\times \sum_{\alpha=\text{TM,TE}} \ln [1 - r_{\alpha}^2(i\zeta_l, y)e^{-y}].$$

Using the variables (35), the reflection coefficients (27) are

$$r_{\text{TM}}(i\zeta_l, y) = \frac{y - Z(i\zeta_l \Omega_c) \zeta_l}{y + Z(i\zeta_l \Omega_c) \zeta_l},$$

$$r_{\text{TE}}(i\zeta_l, y) = \frac{\zeta_l - yZ(i\zeta_l \Omega_c)}{\zeta_l + yZ(i\zeta_l \Omega_c)}. \quad (37)$$

Here, the impedance function of infrared optics (31) is given by

$$Z(i\zeta_l \Omega_c) \equiv Z_i(i\zeta_l \Omega_c) = \frac{\rho \zeta_l}{\sqrt{1 + \rho^2 \zeta_l^2}}, \quad (38)$$

where $\rho \equiv \lambda_p / (4\pi a) = \delta_i / (2a)$ is much less than unity throughout the entire region of application of the impedance approach.

In terms of new variables the Casimir energy at $T = 0$ in Eq. (6) is given by

$$E(a) = \frac{\hbar c}{32\pi^2 a^3} \int_0^{\infty} d\zeta \int_{\zeta}^{\infty} f(\zeta, y) dy \quad (39)$$

and the thermal correction to it (7) by

$$\Delta\mathcal{F}(a, T) = \frac{i\hbar c \kappa}{32\pi^2 a^3} \int_0^{\infty} dt \frac{\Phi(i\kappa t) - \Phi(-i\kappa t)}{e^{2\pi t} - 1}, \quad (40)$$

where the following notations are used:

$$f(\zeta, y) = y \ln [1 - r_{\text{TM}}^2(i\zeta, y)e^{-y}]$$

$$+ y \ln [1 - r_{\text{TE}}^2(i\zeta, y)e^{-y}],$$

$$\Phi(x) \equiv \int_x^{\infty} dy f(x, y). \quad (41)$$

Now, we expand the function f defined in Eq. (41) in powers of the small parameter ρ using Eqs. (37) and (38):

$$f(x, y) = 2y \ln(1 - e^{-y}) + 4\rho \frac{x^2 + y^2}{e^y - 1}$$

$$- 8\rho^2 \frac{(x^4 + y^4)e^y}{y(e^y - 1)^2} + O(\rho^3). \quad (42)$$

Substituting Eq. (42) into the definition of Φ in Eq. (41), we obtain

$$\Phi(x) = I_0(x) + \rho I_1(x) + \rho^2 I_2(x) + O(\rho^3), \quad (43)$$

where

$$I_0(x) = 2 \int_x^{\infty} y dy \ln(1 - e^{-y}),$$

$$I_1(x) = 4 \int_x^{\infty} dy \frac{x^2 + y^2}{e^y - 1}, \quad (44)$$

$$I_2(x) = -8 \int_x^{\infty} dy \frac{(x^4 + y^4)e^y}{y(e^y - 1)^2}.$$

The integrals $I_0(x)$ and $I_1(x)$ are easily calculated [69] and are given by:

$$\begin{aligned} I_0(x) &= -2 \left[\text{Li}_3(e^{-x}) + x \text{Li}_2(e^{-x}) \right] \\ &= -2\zeta(3) + \frac{1}{2}x^2 - x^2 \ln x + \frac{1}{3}x^3 + \text{O}(x^4), \quad (45) \\ I_1(x) &= 8 \left[\text{Li}_3(e^{-x}) + x \text{Li}_2(e^{-x}) - x^2 \ln(1 - e^{-x}) \right] \\ &= 8 \left[\zeta(3) - \frac{1}{4}x^2 - \frac{1}{2}x^2 \ln x + \frac{1}{3}x^3 + \text{O}(x^4) \right], \end{aligned}$$

where $\text{Li}_n(z)$ is the polylogarithm function and $\zeta(x)$ is the Riemann zeta function. As to the integral $I_2(x)$ in Eq. (44), in is easily seen that

$$I_2(x) = -48\zeta(3) + \text{O}(x^4) \quad (46)$$

and, thus, $I_2(x)$ does not contribute to $\Phi(i\kappa t) - \Phi(-i\kappa t)$ in the perturbation orders under consideration.

Substituting Eq. (45) into Eq. (43), we obtain

$$\begin{aligned} \Phi(i\kappa t) - \Phi(-i\kappa t) &= \pi i(\kappa t)^2 - \frac{2}{3}i(\kappa t)^3 \quad (47) \\ &+ 4\rho \left[\pi i(\kappa t)^2 - \frac{4}{3}i(\kappa t)^3 \right] + \text{O}[(\kappa t)^4]. \end{aligned}$$

Now, it is easy to calculate the free energy of the fluctuating field at small κ from Eqs. (5), (39), (40) and (47)

$$\begin{aligned} \mathcal{F}_i(a, T) &= E(a) - \frac{\pi^2 \hbar c}{720a^3} \left[\frac{45\zeta(3)}{8\pi^6} \kappa^3 - \frac{1}{16\pi^4} \kappa^4 \right. \\ &\left. + \frac{45\rho}{\pi^4} \left(\frac{\zeta(3)}{2\pi^2} \kappa^3 - \frac{1}{90} \kappa^4 \right) \right]. \quad (48) \end{aligned}$$

It is convenient to introduce the so-called effective temperature $k_B T_{\text{eff}} = \hbar \Omega_c$ and to use the effective penetration depth of electromagnetic oscillations into a metal (29) in the frequency region of infrared optics, $\delta_i = c/\omega_p = \lambda_p/(2\pi)$. Then, Eq. (48) can be rearranged in the form

$$\begin{aligned} \mathcal{F}(a, T) &= E(a) - \frac{\pi^2 \hbar c}{720a^3} \left\{ \frac{45\zeta(3)}{\pi^3} \left(\frac{T}{T_{\text{eff}}} \right)^3 - \left(\frac{T}{T_{\text{eff}}} \right)^4 \right. \\ &\left. + \frac{\delta_i}{a} \left[\frac{90\zeta(3)}{\pi^3} \left(\frac{T}{T_{\text{eff}}} \right)^3 - 4 \left(\frac{T}{T_{\text{eff}}} \right)^4 \right] \right\}. \quad (49) \end{aligned}$$

In the above, we have restricted our consideration to the second perturbation order in the small parameter ρ . In the same way as in [70] it can be shown that the higher perturbation orders in ρ contain only terms of order $\text{O}(\kappa^n)$ with $n \geq 5$. It is notable that Eq. (49) coincides [39,40] with the free energy of the fluctuating field at low temperatures obtained from the Lifshitz formula combined with the dielectric permittivity of the plasma model $\varepsilon_i(\omega)$ in Eq. (31). Thus, the characterization of a metal by means of the dielectric permittivity and Leontovich surface impedance in the frequency region of infrared optics leads to the same asymptotic behavior of the free energy at low temperatures.

The asymptotic behavior of the entropy of a fluctuating field defined as

$$S(a, T) = -\frac{\partial \mathcal{F}(a, T)}{\partial T} \quad (50)$$

can be found by differentiating Eq. (49)

$$\begin{aligned} S_i(a, T) &= \frac{3k_B}{8\pi a^2} \left(\frac{T}{T_{\text{eff}}} \right)^2 \left[\zeta(3) - \frac{4\pi^3}{135} \frac{T}{T_{\text{eff}}} \right. \\ &\left. + \frac{\delta_i}{a} \left(2\zeta(3) - \frac{16\pi^3}{135} \frac{T}{T_{\text{eff}}} \right) \right]. \quad (51) \end{aligned}$$

As is seen in Eq. (51), entropy goes to zero when temperature vanishes in accordance to the Nernst heat theorem. Thus, the Leontovich impedance of the infrared optics withstands the thermodynamic test. The Lifshitz formulas (1) and (12) combined with the impedance of infrared optics are shown to be consistent with the requirements of thermodynamics.

5 Thermodynamic test for the surface impedance of the Drude model

In the previous section we have extrapolated the impedance function of infrared optics to all lower frequencies, including zero frequency. However, in the Lifshitz formula, Eq. (1), the zero Matsubara frequency is situated outside the region of infrared optics. In a similar manner, small real frequencies in the Lifshitz formula (12) satisfy inequalities (30) and, thus, belong to the region of the normal skin effect. Because of this, it seems reasonable to use the impedance function (33) which coincides with the impedances of infrared optics and of normal skin effect at high and low frequencies, respectively, and provides a smooth analytic interpolation between the two frequency regions. In this section we put the Lifshitz formulas, Eq. (1) and Eq. (12), combined with the impedance of the Drude model (33) to a thermodynamic test.

For $l \geq 1$ one can introduce the dimensionless variable $x_l = \gamma(T)/\xi_l$ and rearrange the impedance of the Drude model (33) in the form

$$Z_D(i\xi_l) = Z_D(i\xi_l \Omega_l) = \frac{\rho \zeta_l}{\sqrt{\rho^2 \zeta_l^2 + \frac{1}{1+x_l}}}. \quad (52)$$

If the relaxation parameter $\gamma(T)$ is equal to zero, $x_l = 0$ and Eq. (52) coincides with Eq. (38) for the impedance of the infrared optics. It is easily seen that for metals with perfect crystal lattices $x_l \ll 1$ at sufficiently low T . In fact, for $T = 300$ K for good metals it holds $\gamma \sim 10^{13} - 10^{14}$ rad/s (as an example, for gold $\gamma = 5.32 \times 10^{13}$ rad/s), whereas $\xi_l = \xi_1 l$ and $\xi_1 = 2\pi k_B T/\hbar = 2.46 \times 10^{14}$ rad/s leading to $x_l = \gamma/\xi_l < 0.22$. When T decreases from $T = 300$ K to approximately $T_D/4$, where T_D is the Debye temperature (for gold $T_D = 165$ K [71]), $\gamma(T)$ decreases linearly, $\gamma(T) \sim T$, i.e., following the same law as ξ_l . At $T < T_D/4$ the relaxation parameter decreases according

to the Bloch-Grüneisen law, $\gamma(T) \sim T^5$, due to electron-phonon collisions [68] and as $\gamma(T) \sim T^2$ at liquid helium temperatures due to electron-electron scattering [71]. At $T = 30$ K and 10 K it holds $\gamma(T)/\xi_1(T) \approx 4.9 \times 10^{-2}$ and 1.8×10^{-3} , respectively. The magnitude of parameter x_l decreases further to zero with $T \rightarrow 0$.

We represent the free energy of the fluctuating field in Eq. (36) in the form

$$\mathcal{F}_D(a, T) = \mathcal{F}_D^{(l=0)}(a, T) + \mathcal{F}_D^{(l \geq 1)}(a, T), \quad (53)$$

where we separate the terms with zero and nonzero Matsubara frequencies. Substituting the impedance function, Eq. (33), in the reflection coefficients, Eq. (37), one obtains

$$r_{\text{TM}}^2(0, y) = r_{\text{TE}}^2(0, y) = 1, \quad (54)$$

which leads to

$$\mathcal{F}_D^{(l=0)}(a, T) = \frac{k_B T}{8\pi a^2} \int_0^\infty y dy \ln(1 - e^{-y}). \quad (55)$$

The contribution from Matsubara frequencies with $l \geq 1$, $\mathcal{F}_D^{(l \geq 1)}(a, T)$, is more cumbersome. We will find its low-temperature asymptotic behavior perturbatively. With this purpose we expand Z_D in Eq. (52) in powers of a small parameter x_l

$$\begin{aligned} Z_D(i\zeta_l \Omega_c) &= \frac{\rho\zeta_l}{\sqrt{1 + \rho^2\zeta_l^2}} + \frac{(\rho\zeta_l)^{-2}x_l}{2[1 + (\rho\zeta_l)^{-2}]^{3/2}} + \text{O}(x_l^2) \\ &= Z_i(i\zeta_l \Omega_c) + \tilde{x}_l + \text{O}(x_l^2), \end{aligned} \quad (56)$$

where the impedance of infrared optics, Z_i , is defined in Eq. (38) and

$$\tilde{x}_l \equiv \frac{\gamma(T)}{2\omega_p} (1 + \rho^2\zeta_l^2)^{-3/2} \ll 1. \quad (57)$$

Now, we substitute Eq. (56) in Eq. (36) with omitted zero-frequency contribution and expand $\mathcal{F}_D^{(l \geq 1)}(a, T)$ in powers of \tilde{x}_l keeping only the first order term:

$$\begin{aligned} \mathcal{F}_D^{(l \geq 1)}(a, T) &= \mathcal{F}_i^{(l \geq 1)}(a, T) + \frac{k_B T}{2\pi a^2} \sum_{l=1}^\infty \zeta_l \tilde{x}_l \\ &\times \int_{\zeta_l}^\infty y^2 dy e^{-y} \left\{ \frac{-y + \zeta_l Z_i(i\zeta_l \Omega_c)}{A_{\text{TM}}} + \frac{\zeta_l - y Z_i(i\zeta_l \Omega_c)}{A_{\text{TE}}} \right\} \\ &+ \text{O}(\tilde{x}_l^2), \end{aligned} \quad (58)$$

where

$$\begin{aligned} A_{\text{TM}} &= [y + \zeta_l Z_i(i\zeta_l \Omega_c)] \\ &\times [(e^{-y} - 1)(y^2 + \zeta_l^2 Z_i^2(i\zeta_l \Omega_c)) \\ &\quad - 2(e^{-y} + 1)\zeta_l y Z_i(i\zeta_l \Omega_c)], \\ A_{\text{TE}} &= [\zeta_l + y Z_i(i\zeta_l \Omega_c)] \\ &\times [(e^{-y} - 1)(\zeta_l^2 + y^2 Z_i^2(i\zeta_l \Omega_c)) \\ &\quad - 2(e^{-y} + 1)\zeta_l y Z_i(i\zeta_l \Omega_c)]. \end{aligned}$$

Here $\mathcal{F}_i^{(l \geq 1)}(a, T)$ is the free energy of the fluctuating field, computed by using the impedance of infrared optics

(38), with omitted contribution from the zero Matsubara frequency. As a next step, we expand the integrand in Eq. (58) in powers of a small impedance of infrared optics, $Z_i(i\zeta_l \Omega_c)$, and retain only the zero order contribution [recall that $Z_i(i\zeta_l \Omega_c)$ goes to zero when T vanishes]:

$$\begin{aligned} \mathcal{F}_D^{(l \geq 1)}(a, T) &= \mathcal{F}_i^{(l \geq 1)}(a, T) \\ &+ \frac{k_B T}{2\pi a^2} \sum_{l=1}^\infty \tilde{x}_l \int_{\zeta_l}^\infty \frac{dy}{1 - e^y} \left(-\zeta_l + \frac{y^2}{\zeta_l} \right) \\ &+ \text{O} [Z_i(i\zeta_l \Omega_c) \tilde{x}_l, \tilde{x}_l^2]. \end{aligned} \quad (59)$$

Bearing in mind the definition of \tilde{x}_l in Eq. (57), the sum in Eq. (59) takes the form

$$\Sigma = \frac{\gamma(T)}{2\omega_p} \sum_{l=1}^\infty (1 + \rho^2\zeta_l^2)^{-3/2} \int_{\zeta_l}^\infty \frac{dy}{1 - e^y} \left(-\zeta_l + \frac{y^2}{\zeta_l} \right). \quad (60)$$

Now we expand the integrand in Eq. (60) in powers of e^{-y} and introduce the new variable $v = jy$, where $j = 1, 2, 3, \dots$. Thus, we obtain

$$\Sigma = \frac{\gamma(T)}{2\omega_p} \sum_{l=1}^\infty (1 + \rho^2\zeta_l^2)^{-3/2} \sum_{j=1}^\infty \frac{1}{j} \int_{j\zeta_l}^\infty dv e^{-v} \left(\zeta_l - \frac{v^2}{j^2\zeta_l} \right). \quad (61)$$

After the integration with respect to v , this leads to

$$\Sigma = -\frac{\gamma(T)}{\omega_p} \sum_{l=1}^\infty (1 + \rho^2\zeta_l^2)^{-3/2} \sum_{j=1}^\infty \frac{1}{j^2} \left(\frac{1}{j\zeta_l} + 1 \right) e^{-j\zeta_l}. \quad (62)$$

By expanding in powers of $\rho\zeta_l \equiv \rho\kappa l$ and performing the summation in l we obtain

$$\begin{aligned} \Sigma &= \frac{\gamma(T)}{\omega_p} \left\{ \frac{1}{\kappa} \sum_{j=1}^\infty \frac{1}{j^3} \ln(1 - e^{-j\kappa}) - \sum_{j=1}^\infty \frac{1}{j^2(e^{j\kappa} - 1)} \right. \\ &+ \left. \frac{3}{2} \rho^2 \kappa^2 \left[\frac{1}{\kappa} \sum_{j=1}^\infty \frac{e^{-j\kappa}}{j^3(1 - e^{-j\kappa})^2} + \sum_{j=1}^\infty \frac{e^{-j\kappa}(1 + e^{-j\kappa})}{j^2(1 - e^{-j\kappa})^3} \right] \right. \\ &+ \left. \text{O}(\rho^4 \kappa^4) \right\}. \end{aligned} \quad (63)$$

In the asymptotic limit $\kappa \rightarrow 0$, Eq. (63) results in

$$\Sigma \approx \frac{\gamma(T)}{\omega_p} \frac{\ln \kappa}{\kappa} \zeta(3) + \frac{\gamma(T)}{\omega_p} \text{O} \left(\frac{1}{\kappa} \right). \quad (64)$$

The substitution of this expression into Eq. (59) leads to

$$\begin{aligned} \mathcal{F}_D^{(l \geq 1)}(a, T) &= \mathcal{F}_i^{(l \geq 1)}(a, T) + \frac{k_B T \gamma(T)}{2\pi a^2 \omega_p} \frac{\ln \kappa}{\kappa} \zeta(3) \\ &+ \text{O} [Z_i(i\zeta_l \Omega_c) \tilde{x}_l, \tilde{x}_l^2] + \frac{k_B T \gamma(T)}{2\pi a^2 \omega_p} \text{O} \left(\frac{1}{\kappa} \right). \end{aligned} \quad (65)$$

Now we are in a position to find the asymptotic expression at small κ for the free energy computed using the impedance of the Drude model. First we add the zero-frequency term $\mathcal{F}_D^{(l=0)}(a, T)$, defined in Eq. (55), to both

sides of Eq. (65). On the left-hand side of this equation the quantity $\mathcal{F}_D(a, T)$ is obtained. On the right-hand side of Eq. (65) we add and subtract the zero-frequency term of the free energy computed using the impedance of the plasma model. This term is obtained from Eqs. (36)–(38):

$$\begin{aligned} \mathcal{F}_i^{(l=0)}(a, T) &= \frac{k_B T}{16\pi a^2} \int_0^\infty y dy \left\{ \ln(1 - e^{-y}) \right. \\ &\quad \left. + \ln \left[1 - \left(\frac{1 - \rho y}{1 + \rho y} \right)^2 e^{-y} \right] \right\}. \end{aligned} \quad (66)$$

The term (66), together with the first term on the right-hand side of Eq. (65), gives us the free energy $\mathcal{F}_i(a, T)$ computed using the impedance of infrared optics. As a result, from Eq. (65) it follows:

$$\begin{aligned} \mathcal{F}_D(a, T) &= \mathcal{F}_i(a, T) + \Delta\mathcal{F}_i^{(l=0)}(a, T) \\ &\quad + \frac{k_B T \gamma(T)}{2\pi a^2 \omega_p} \frac{\ln \kappa}{\kappa} \zeta(3) + \mathcal{O} [Z_i(i\zeta_l \Omega_c) \tilde{x}_l, \tilde{x}_l^2] \\ &\quad + \frac{k_B T \gamma(T)}{2\pi a^2 \omega_p} \mathcal{O} \left(\frac{1}{\kappa} \right), \end{aligned} \quad (67)$$

where

$$\begin{aligned} \Delta\mathcal{F}_i^{(l=0)}(a, T) &= \mathcal{F}_D^{(l=0)}(a, T) - \mathcal{F}_i^{(l=0)}(a, T) \quad (68) \\ &= \frac{k_B T}{16\pi a^2} \int_0^\infty y dy \left\{ \ln(1 - e^{-y}) \right. \\ &\quad \left. - \ln \left[1 - \left(\frac{1 - \rho y}{1 + \rho y} \right)^2 e^{-y} \right] \right\} \\ &= -\frac{k_B T}{16\pi a^2} \left\{ \zeta(3) \right. \\ &\quad \left. + \int_0^\infty y dy \ln \left[1 - \left(\frac{1 - \rho y}{1 + \rho y} \right)^2 e^{-y} \right] \right\}. \end{aligned}$$

Taking into account that $\kappa \sim T$ and at low temperatures $\gamma(T) \sim T^2$, $Z_i(i\zeta_l \Omega_c) \sim T$, $\tilde{x}_l \sim \gamma \sim T^2$, we arrive at the conclusion that not only the last three terms on the right-hand side of Eq. (67) vanish when temperature vanishes, but also their derivatives with respect to temperature vanish.

Using Eq. (50), we can find the asymptotic behavior of the free energy and entropy of the fluctuating field at low temperatures in the case that the metal is described by the impedance of the Drude model. Keeping only the main terms of order T and $T^2 \ln T$ in Eq. (67) [recall that according to Eq. (49) $\mathcal{F}_i(a, T) - E(a) \sim T^3$], we obtain

$$\begin{aligned} \mathcal{F}_D(a, T) &= E(a) + \Delta\mathcal{F}_i^{(l=0)}(a, T) \\ &\quad + \frac{k_B T \gamma(T)}{2\pi a^2 \omega_p} \frac{\ln \kappa}{\kappa} \zeta(3), \quad (69) \\ S_D(a, T) &= -\frac{\partial \Delta\mathcal{F}_i^{(l=0)}(a, T)}{\partial T} \end{aligned}$$

$$\begin{aligned} &- \frac{k_B \zeta(3)}{2\pi^2 a^2} \frac{\gamma(T)}{\omega_p} \frac{T_{\text{eff}}}{T} \left(\ln \kappa + \frac{1}{2} \right) \\ &= \frac{k_B}{16\pi a^2} \left\{ \zeta(3) + \int_0^\infty y dy \ln \left[1 - \left(\frac{1 - \rho y}{1 + \rho y} \right)^2 e^{-y} \right] \right\} \\ &\quad - \frac{k_B \zeta(3)}{2\pi^2 a^2} \frac{\gamma(T)}{\omega_p} \frac{T_{\text{eff}}}{T} \left[\ln \left(2\pi \frac{T}{T_{\text{eff}}} \right) + \frac{1}{2} \right]. \end{aligned}$$

Expanding the integrand on the right-hand side of the second equality in Eq. (69) in powers of ρ and integrating with respect to y , we arrive at

$$\begin{aligned} S_D(a, T) &= \frac{k_B \zeta(3)}{2\pi a^2} \rho [1 - 6\rho + \mathcal{O}(\rho^2)] \quad (70) \\ &\quad - \frac{k_B \zeta(3)}{2\pi^2 a^2} \frac{\gamma(T)}{\omega_p} \frac{T_{\text{eff}}}{T} \left[\ln \left(2\pi \frac{T}{T_{\text{eff}}} \right) + \frac{1}{2} \right]. \end{aligned}$$

To carry out the thermodynamic test of the impedance of the Drude model, we consider T approaching zero and find the following value of the entropy:

$$\begin{aligned} S_D(a, 0) &= \frac{k_B}{16\pi a^2} \left\{ \zeta(3) \right. \\ &\quad \left. + \int_0^\infty y dy \ln \left[1 - \left(\frac{1 - \rho y}{1 + \rho y} \right)^2 e^{-y} \right] \right\} \\ &= \frac{k_B \zeta(3)}{2\pi a^2} \rho [1 - 6\rho + \mathcal{O}(\rho^2)] > 0. \quad (71) \end{aligned}$$

As is seen from Eq. (71), the entropy of the fluctuating field at zero temperature takes a nonzero positive value. This value depends on the parameters of the system, i.e., on the separation distance a , and on the plasma frequency ω_p . The latter participates through the definition of ρ (recall that for metals without impurities described by ε_D the Casimir entropy at $T = 0$ is negative [39, 40]). What this means is that we have a violation of the third law of thermodynamics, the Nernst heat theorem [72].

In the above calculations we have considered the entropy associated with the fluctuating field. In other words, only the distance dependent part of the total free energy was considered. However, inclusion of the self-energies cannot invalidate our conclusion on the violation of the Nernst heat theorem. The reason is that the entropy of a fluctuating field in Eq. (71) depends on the separation distance, whereas the entropies due to self-energies are separation independent. As a consequence, the entropy of a fluctuating field and the entropies of matter fields cannot cancel each other and must satisfy the Nernst heat theorem separately.

Thus, the Leontovich impedance of the Drude model is thermodynamically inconsistent and cannot be used in combination with the Lifshitz formulas, Eq. (1) and Eq. (12), to calculate the thermal Casimir force. In the next section it is also shown that the thermal Casimir force computed using the impedance of the Drude model is in disagreement with the experimental data of [17]. Thus, there are both theoretical and experimental evidences against the use of this impedance function in the theory of the thermal Casimir force.

6 Alternative results for the thermal correction to the Casimir pressure computed with different impedance functions

In [57,58] the contribution from the transverse electric electromagnetic waves to the thermal correction $\Delta P(a, T)$ was computed using the real frequency axis formalism and the impedance function of the normal skin effect $Z_N(\omega)$ defined in Eq. (32). The computation was performed for Au plates at room temperature with static conductivity $\sigma_0 = 3 \times 10^{17} \text{ s}^{-1}$ and relaxation time $\tau = 1.88 \times 10^{-14} \text{ s}$. As was noted in Sec. 3, the impedance function (32) can be obtained from the dielectric function in the region of the normal skin effect, $\varepsilon_N(\omega)$, using Eq. (26) where the static conductivity is connected with the plasma frequency ω_p by Eq. (34) leading to $\omega_p \approx 9.3 \text{ eV}$. In [57,58] the relatively large contribution to the thermal correction from the TE waves for plates separation $a = 1 \mu\text{m}$ was obtained using the impedance function (32). It is about 30 times larger than the corresponding correction for ideal metals. This was explained by the increased role of the TE EW at low frequencies. According to [59] the predicted increase of the thermal correction at $a = 1 \mu\text{m}$ is in conflict with previous theoretical work [37] that predicts even several times larger magnitudes for the thermal correction calculated using the dielectric permittivity $\varepsilon \sim \omega^{-1}$ at low frequencies. Paper [59] concludes also that the prediction of [57,58] is consistent with the experimental data of [9] at $a = 1 \mu\text{m}$ whereas the prediction of [37] is excluded by that experiment.

Here we repeat the numerical computations of [57,58] for the contribution of the TE mode to the thermal correction to the Casimir force, using the impedance (32). We also compute the contribution from the TM mode and study the role of EW and PW in both contributions. The computations are performed at different separations using both formalisms along the imaginary and real frequency axis (presented in Secs. 2 and 3) with practically coinciding results. Although the thermal correction predicted from the impedance (32) is consistent with the long-separation experiment [9] at $1 \mu\text{m}$, it is shown to be excluded by the measurement of the Casimir force at shorter separations by means of the micromechanical torsional oscillator [17,18,19,20]. Because of this, we also discuss several other forms of impedance function and find those consistent with experiment.

For the purpose of comparison with experiment (which is in fact consistent with the theoretical results for $P_0(a)$ at $T = 0$ [17]), here we use in computations slightly different value of the plasma frequency $\omega_p = 9.0 \text{ eV}$. The thermal correction in the framework of the imaginary frequency axis formalism was computed by Eqs. (2), (5) and (9) for two similar Au plates at $T = 300 \text{ K}$. The results are presented in Table 1 where column 1 contains the values of the separation distance between the plates and column 2 the values of the thermal correction. Precisely the same values were computed using Eq. (18) of the real frequency axis formalism. Note that although the magnitude of the thermal correction increases with

the decrease of separation, the relative thermal correction becomes smaller at shorter separations. The same holds for metals described by the dielectric permittivity of the plasma model [34,35]. In column 3 of Table 1 the ratios of the thermal correction from column 2 to those for ideal metal (denoted by $\Delta P_{\text{TE}}^{\text{IM}}$) are presented. Columns 4 and 5 contain the relative contributions to the thermal correction from the TE EW and PW, respectively, computed by using Eqs. (20) and (21). In columns 6 and 7 the relative contributions from the TM EW and PW, respectively, are presented. Here and below we perform all computations at $a \geq 200 \text{ nm}$ in order to remain well inside the application region of the impedance approach. For example, at $a = 200 \text{ nm}$ the characteristic frequency of the Casimir force is $\omega_c = c/(2a) \approx 7.5 \times 10^{14} \text{ rad/s}$ and $Z_N(\omega_c) \approx 1.4 \times 10^{-2} \ll 1$. As is seen from columns 2 and 3 in Table 1, the magnitudes of the total thermal correction computed with the impedance function (32) are rather large. At separation distance of $1 \mu\text{m}$ the thermal correction for Au plates is found to be almost 16 times larger than for the plates made of ideal metal. This ratio quickly increases with the decrease of separation. At a separation of 200 nm it is as large as 5900. By the summation of the values presented in columns 4,5 from one hand and 6,7 from another hand, one finds that the dominant contributions to ΔP are given by the TE mode, whereas the relative contributions from the TM mode are negligibly small. The largest value of the latter achieved at $a = 1 \mu\text{m}$ is equal to 0.05. Comparing columns 4 and 5 from one hand and 6 and 7 from another, we can conclude that the dominant contribution to ΔP_{TE} and ΔP_{TM} is given by the EW. If one considers only the contribution from the TE mode discussed in [57], one obtains $\Delta P_{\text{TE}}/\Delta P_{\text{TE}}^{\text{IM}} = 29.6$ and 1.2×10^4 at separations $a = 1 \mu\text{m}$ and $0.2 \mu\text{m}$, respectively.

Now we compare the obtained magnitudes of the thermal correction in column 2 of Table 1 with the experiment [17]. For this purpose we need to obtain the total magnitudes of the Casimir pressure at temperature $T = 300 \text{ K}$. The magnitudes of $P_0(a)$ can be most simply computed using Eqs. (9) and (27). However, use of the impedance function (32) leads to incorrect values of $P_0(a)$. As an example, using (32) one obtains $|P_0| = 716.5$ and 144.6 mPa at separations 200 nm and 300 nm , respectively. At the same time, the conventional magnitudes of P_0 at these separations, obtained by different authors [76,77,78] are 507.5 and 113.6 mPa , respectively, in drastic contradiction with the above values obtained by the use of impedance (32). The reason is that the dominant contribution to P_0 is given by the frequency region around the characteristic frequency ω_c which belongs not to the region of the normal skin effect, where the impedance function (32) is appropriate, but to the region of infrared optics. On the contrary, the magnitude of the thermal correction (18) with the impedance function (32) is determined by much lower frequencies where (32) is applicable.

To compare the thermal correction in column 2 of Table 1 with experiment, we add it to the conventional magnitudes of the Casimir pressure at $T = 0$ specified above.

As a result, at separations 200 and 300 nm one obtains the magnitudes of the thermal Casimir pressure equal to 519.6 and 116.4 mPa, respectively. These should be compared with respective measured magnitudes of the Casimir pressure at the same separations equal to 508.1 and 114.7 mPa. The differences between the above theoretical and experimental values are 11.5 and 1.7 mPa. They lie outside the boundary of the half-width confidence interval determined at 95% confidence (at separations 200 and 300 nm the latter is equal to 8.6 and 1.6 mPa, respectively). Thus, the impedance function (32) is not consistent with the measurement of the Casimir pressure at short separations by means of micromechanical torsional oscillator [17, 18, 19, 20].

The impedance Z_N is applicable only at low frequencies specific for the normal skin effect. As was discussed in Sec. 3, the impedance of the Drude model (33) provides smooth interpolation between the regions of the normal skin effect and infrared optics. At all frequencies $\omega \ll \omega_p$ the impedance (33) can be represented in the form (32) if one replaces σ_0 on the right-hand side of (32) by the ac conductivity defined as

$$\sigma(\omega) = \frac{\sigma_0}{1 - i\tau\omega}. \quad (72)$$

It is easily seen that the impedance of the Drude model (33) leads to even larger magnitudes for the thermal correction to the Casimir pressure at short separations, than the impedance (32). At the separation $a = 0.2 \mu\text{m}$ the magnitude of the thermal correction computed with the impedance (33) is equal to $|\Delta P| = 14.7 \text{ mPa}$ and its ratio to the thermal correction for ideal metals is 7200. At $a = 1 \mu\text{m}$ one obtains $|\Delta P| = 0.0402 \text{ mPa}$ and $\Delta P/\Delta P^{\text{ID}} = 20$. If one considers only the contribution from the TE mode, one obtains $\Delta P_{\text{TE}}/\Delta P_{\text{TE}}^{\text{ID}} = 37.4$ (close to 36.5 obtained in [58] for a bit different value of $\omega_p = 9.3 \text{ eV}$ whereas in our computations here we use $\omega_p = 9.0 \text{ eV}$). However, at $a \approx 200 \text{ nm}$ this ratio achieves the value $\Delta P_{\text{TE}}/\Delta P_{\text{TE}}^{\text{ID}} \approx 14.3 \times 10^3$. As in the case of impedance function (32), the increase of the thermal correction is due to the contribution from the TE EW.

In the same way, as before, it can be shown that the large thermal correction predicted by the impedance (33) is excluded experimentally. Thus, the theoretical magnitudes of the Casimir pressure obtained by adding the thermal correction to P_0 are equal to 522.15 and 116.99 mPa at separations 200 and 300 nm, respectively. By comparing this with experiment we get the respective differences 14.06 and 2.32 mPa which are far outside the boundary of the 95% confidence interval presented above. [Notice that the use of the Drude dielectric function from Eq. (33) with reflection coefficients (22) to compute the thermal Casimir force is inconsistent not only with experiment [9] but with experiments [16, 17, 18, 19, 20] as well.]

Bearing in mind that in the separation range from 200 nm to $1 \mu\text{m}$ the characteristic frequency $\Omega_c = c/(2a)$ belongs to the region of infrared optics, it is reasonable to calculate the thermal correction to the Casimir pressure using the impedance Z_i defined in Eq. (31). Note that the dielectric permittivity $\varepsilon_i(\omega)$ with the reflection coefficients

(22) was first used to calculate the thermal Casimir pressure in [34, 35]. It was shown that the dielectric permittivity of the plasma model leads to small thermal corrections to the Casimir pressure at short separations in qualitative agreement with the case of ideal metals. At large separations it leads to the same result as for ideal metals in accordance to the classical limit [73, 74].

The disadvantage of the impedance function (31) is that it has zero real part at nonzero frequencies, i.e., does not take relaxation processes into account. At the same time the tabulated optical data for the complex index of refraction n in the region of infrared optics [75] lead to a nonzero real part of the impedance function which, however, is much less than the magnitude of the imaginary part. Unfortunately, the optical data at low frequencies are not available. In addition, these data are burdened by large errors and uncertainties. Because of this, any theoretical result for the functional form of the impedance function is of much value. Preserving only the first expansion orders for both real and imaginary parts, a more accurate complex impedance in the region of the infrared optics can be approximately presented in the form [51]

$$Z_p(\omega) = C\omega^2 - i \frac{\omega}{\sqrt{\omega_p^2 - \omega^2}}, \quad (73)$$

where the constant $C = 0.004 \text{ eV}^{-2}$ was chosen to provide the best mean fit to the optical data for the real part of the impedance within the frequency region from 0.125 eV to 5 eV. The impedance (73) disregards interband transitions but the real part of it takes into account electron-electron collisions which occur rather seldom in the region of infrared optics.

In Fig. 1 the imaginary (a) and real (b) parts of the impedance (73) are shown by the solid lines as functions of the frequency. In the same figure the imaginary (a) and real (b) parts of the impedance are plotted by dots using the expression $Z_p(\omega) = 1/n(\omega)$ and the tabulated optical data for $n(\omega)$ [75]. As is seen in Fig. 1b, in the region $\omega \leq 1.5 \text{ eV}$ the analytic expression for the imaginary part of the impedance (73) is in rather good agreement with data. This expression gives the major contribution to the impedance along the imaginary frequency axis

$$Z_p(i\xi) = -C\xi^2 + \frac{\xi}{\sqrt{\omega_p^2 + \xi^2}}. \quad (74)$$

Then one can conclude that the approximation (74) is well adapted for the computation of the thermal correction to the Casimir pressure.

The computations were performed for Au plates by using both the imaginary and real frequency axis formalisms discussed in Sec. 2 with practically coinciding results for the total thermal correction and also for separate contributions from the TE and TM modes. When using the real frequency formalism, some care is necessary in the numerical integration of Eqs.(20) and (21), because, due to the smallness of the real part of Z_i , there exist narrow resonances in the spectrum of the thermal correction, corresponding to the eigenfrequencies of a dissipationless cavity

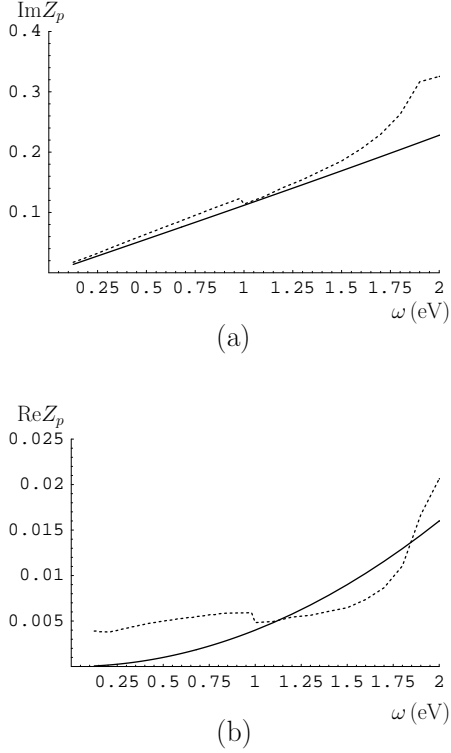


Fig. 1. Imaginary (a) and real (b) parts of the impedance of infrared optics as functions of frequency. Solid lines are for the analytical expression (73), dots correspond to the tabulated optical data.

with impedance $Z_i(\omega)$. These considerations apply especially to the computation $\Delta P_{\text{TM,EW}}$, because its spectrum has resonances also at thermal frequencies. These results are presented in Table 2. In column 2 the magnitudes of the total thermal correction to the Casimir pressure at different separations are listed. Column 3 contains the ratios of the total thermal corrections for Au plates to those for ideal metals. In column 4 the relative contributions from the TE EW to the total thermal correction are shown. Column 5 contains the relative contributions from the TE PW to the total thermal correction. Columns 6 and 7 contain the relative contributions to the total thermal correction from the TM EW and TM PW, respectively. As is seen from columns 2 and 3 in Table 2, the impedance of infrared optics leads to much smaller thermal corrections than the impedance of the normal skin effect in qualitative agreement with the case of ideal metals. From columns 4–7 it follows that the TE and TM modes lead to qualitatively similar contributions. The role of EW is also not so pronounced as it was for the impedance of the normal skin effect.

The total thermal Casimir pressures obtained by the summation of the thermal corrections in column 2 of Table 2 and zero-temperature pressures are consistent with all available experimental data. By way of example, at $a = 200$ and 300 nm (where for the impedance of the nor-

mal skin effect the theoretical results were excluded at 95% confidence) the differences between theory and experiment [17,18] are now equal to -0.61 and -1.1 mPa, respectively, i.e., well inside the 95% confidence interval. Note that the thermal Casimir force computed using the dielectric permittivity (31) is also consistent with data [17]. The addition of a small imaginary part to $\varepsilon_i(\omega)$, arising from real part of the impedance in Eq. (73), leads to only minor changes in the computation results which remain consistent with experiment.

Thus, the impedance of infrared optics (74) leads to reasonable results when applied to the thermal Casimir pressure. In the following sections we are going to apply the impedance method to the computation of the radiative heat transfer across a vacuum gap between two parallel surfaces at different temperatures. As is shown in Sec. 7 below, this process is mostly determined by the real part of the impedance function which is modelled not enough precisely in Eq. (73) (see Fig. 1b). Bearing in mind the computations of the radiative heat transfer, we introduce one more model impedance of infrared optics by the equation

$$Z_t(\omega) = \left\{ \begin{array}{ll} B \sin\left(\frac{\pi\omega^2}{2\beta^2}\right), & \omega \leq \beta, \\ B, & \beta \leq \omega \leq 0.125 \text{ eV}, \\ Y(\omega), & \omega \geq 0.125 \text{ eV} \end{array} \right\} - i \frac{\omega}{\sqrt{\omega_p^2 - \omega^2}}. \quad (75)$$

Here $Y(\omega)$ stands for the tabulated optical data representing the real part of the impedance [75] which are available at $\omega \geq 0.125$ eV. The value of the constant $B = 0.00389$ is chosen such as to have a smooth transition between the optical data and their extrapolation to lower frequencies. The unknown parameter β fixes the value of frequency where the behavior of $\text{Re}Z_t$, as given by the optical data, is smoothly connected with the asymptotic behavior at low frequencies. The upper bound of β is determined by the fact that the optical data are available at $\omega \geq 0.125$ eV. In the frequency region of infrared optics the real part must be much smaller than the imaginary. The reason is that at these frequencies electrons are almost free and electric current is pure imaginary. The small real part of the impedance describes minor distortions in the vibrational motion of electrons. Then it is reasonable to impose the lower constraint on β as follows: $0.08 \text{ eV} \leq \beta$. This constraint is very conservative because it allows the real part of the impedance to become as large as one half of the imaginary part (a larger real part of the impedance in the region of infrared optics is evidently inadmissible). The real part of the impedance (75) as a function of frequency is shown in Fig. 2, where line 1 corresponds to $\beta = 0.125$ eV and line 2 to $\beta = 0.08$ eV. The region between lines 1 and 2 is allowed.

7 Heat transfer across an empty gap

We consider now the case of two semi-infinite plane parallel metallic plates at different temperatures $T_1 > T_2$,

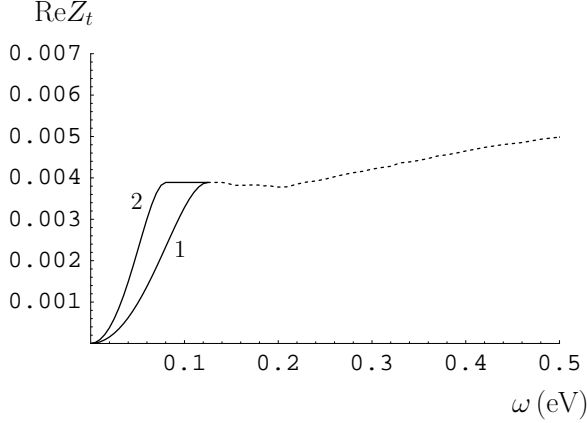


Fig. 2. Real part of the impedance of infrared optics given by the tabulated optical data (dots) versus frequency with different extrapolations to low frequencies (the region between the solid lines 1 and 2). See text for further discussion.

separated by an empty gap of width a . We are interested in estimating the heat transfer between the plates. This problem was first studied long ago by Rytov [79], and later on it was reconsidered by Polder and Van Hove [60], by Loomis and Maris [61] and by Volokitin and Persson [32]. Recently, it was studied by one of us [33] in the framework of the surface impedance. The approach followed by Polder and Van Hove is closely related to Lifshitz theory of the van der Waals interactions between macroscopic bodies, in that heat transfer is regarded as occurring via fluctuating electromagnetic fields radiated by the two plates, whose sources are the random thermal electric currents that are present inside the plates. The fluctuation-dissipation theorem is then used to determine the statistical properties of the currents, from which the correlation properties of the emitted electromagnetic fields are subsequently derived. In the derivation, Polder and Van Hove made the following assumptions, that are also at the basis of Lifshitz theory: i) the wavelengths of the electromagnetic fields involved should be large compared to atomic distances, so that the fluctuating fields can be well described by means of the classical macroscopic Maxwell's equations; ii) the electric currents at distinct points inside the plates are uncorrelated; iii) the media are isotropic and nonmagnetic, and such that their electromagnetic properties can be described by means of a complex dielectric permittivity $\varepsilon(\omega)$ that depends only on the frequency; iv) the system is stationary in time, and each plate is in local thermal equilibrium. The resulting expression for the power (per unit area) S of heat transfer from plate one to plate two, was found using the average value of the Poynting vector in the gap between two plates [61]:

$$S = \frac{4\hbar}{\pi^2} \int_0^\infty d\omega \omega \int_0^\infty dk_\perp k_\perp k_z^2 |e^{2ik_z a}| \quad (76)$$

$$\times \left(\frac{1}{\exp(\hbar\omega/k_B T_1) - 1} - \frac{1}{\exp(\hbar\omega/k_B T_2) - 1} \right)$$

$$\times \left[\frac{\text{Re}(s^{(1)}) \text{Re}(s^{(2)})}{X_{\text{TE}}} + \frac{\text{Re}(\bar{\varepsilon}^{(1)} s^{(1)}) \text{Re}(\bar{\varepsilon}^{(2)} s^{(2)})}{X_{\text{TM}}} \right],$$

where

$$X_{\text{TE}} = |(k_z + s^{(1)})(k_z + s^{(2)}) - (k_z - s^{(1)})(k_z - s^{(2)})e^{2ik_z a}|^2,$$

$$X_{\text{TM}} = |(\varepsilon^{(1)} k_z + s^{(1)})(\varepsilon^{(2)} k_z + s^{(2)}) - (\varepsilon^{(1)} k_z - s^{(1)})(\varepsilon^{(2)} k_z - s^{(2)})e^{2ik_z a}|^2,$$

and

$$s^{(n)}(\omega, k_\perp) = \sqrt{\varepsilon^{(n)}(\omega) \omega^2 / c^2 - k_\perp^2} = ik^{(n)}(\omega, k_\perp) \quad (77)$$

(note that our variable k_\perp is denoted by q in [32, 61]). We now decompose S as the sum of the contributions from PW and EW:

$$S = S_{\text{PW}} + S_{\text{EW}}. \quad (78)$$

It is not hard to verify, starting from Eq. (76), that S_{PW} and S_{EW} can be expressed in terms of the dielectric reflection coefficients (24) as [32]:

$$S_{\text{PW}} = \frac{\hbar}{4\pi^2} \int_0^\infty d\omega \omega \int_0^{\omega/c} dk_z k_z \quad (79)$$

$$\times \left(\frac{1}{\exp(\hbar\omega/k_B T_1) - 1} - \frac{1}{\exp(\hbar\omega/k_B T_2) - 1} \right)$$

$$\times \sum_{\alpha=\text{TE, TM}} \frac{[1 - |r_\alpha^{(1)}(\omega, k_\perp)|^2][1 - |r_\alpha^{(2)}(\omega, k_\perp)|^2]}{|1 - r_\alpha^{(1)}(\omega, k_\perp)r_\alpha^{(2)}(\omega, k_\perp)\exp(2ik_z a)|^2},$$

$$S_{\text{EW}} = \frac{\hbar}{\pi^2} \int_0^\infty d\omega \omega \int_0^\infty dq q \quad (80)$$

$$\times \left(\frac{1}{\exp(\hbar\omega/k_B T_1) - 1} - \frac{1}{\exp(\hbar\omega/k_B T_2) - 1} \right)$$

$$\times \sum_{\alpha=\text{TE, TM}} \frac{\text{Im}r_\alpha^{(1)}(\omega, k_\perp) \text{Im}r_\alpha^{(2)}(\omega, k_\perp) e^{-2qa}}{|1 - r_\alpha^{(1)}(\omega, k_\perp)r_\alpha^{(2)}(\omega, k_\perp)\exp(-2qa)|^2}.$$

It is to be noted that, for $r_\alpha^{(2)} = 0$, $S_{\text{EW}} = 0$, while for $r_\alpha^{(2)} = 0$, and $T_2 = 0$ the expression for S_{PW} reduces to the well known Kirchhoff's formula for the flux of radiation Φ from a surface with reflection coefficients $r_\alpha = r_\alpha^{(1)}$, at temperature $T = T_1$:

$$\Phi(T) = \frac{1}{4\pi^2 c^2} \int_0^\infty d\omega \frac{\hbar\omega^3}{\exp(\hbar\omega/k_B T) - 1}$$

$$\times \int_0^1 dp p \sum_{\alpha=\text{TE, TM}} (1 - |r_\alpha|^2), \quad (81)$$

where $p = k_z c/\omega$.

In [33] the power of heat transfer per unit area S was computed within a general theory of electromagnetic fluctuations for metallic surfaces, based on the concept of surface impedance. This approach is closer to that originally followed by Rytov [79], in that the starting point of the theory is an expression for the correlators of the electric and magnetic fields. However, according to the dictate of

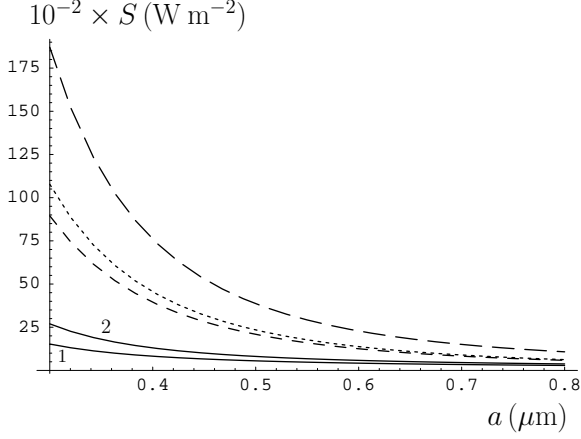


Fig. 3. Plots of radiative heat transfer between two Au plates at temperatures $T_1 = 320$ K and $T_2 = 300$ K, as a function of separation, according to Lifshitz theory for $\varepsilon = \varepsilon_D$ (short-dashed line), and to impedance theory for three different choices of impedance: $Z = Z_N$ (long-dashed line), $Z = Z_D$ (dotted line) and $Z = Z_t$ (band between the solid lines 1 and 2). See text for further explanation.

impedance theory, in [33] the correlators are given only *outside* the metal, while no consideration is made of either the fields, or the electric currents in the *interior* of the metal. The resulting expression for the heat transfer that was found in [33] is:

$$S = \frac{4\hbar c^2}{\pi^2} \int_0^\infty \frac{d\omega}{\omega} \text{Re}Z^{(1)}(\omega) \text{Re}Z^{(2)}(\omega) \times \left(\frac{1}{\exp(\hbar\omega/k_B T_1) - 1} - \frac{1}{\exp(\hbar\omega/k_B T_2) - 1} \right) \times \int_0^\infty dk_\perp k_\perp |k_z|^2 |e^{2ik_z a}| \left(\frac{1}{B_{TE}} + \frac{1}{B_{TM}} \right), \quad (82)$$

where the quantities $B_{TE/TM}$ are defined as:

$$B_{TE} = |(1 + k_z c Z^{(1)}/\omega)(1 + k_z c Z^{(2)}/\omega) - (1 - k_z c Z^{(1)}/\omega)(1 - k_z c Z^{(2)}/\omega) \exp(2ik_z a)|^2, \quad (83)$$

$$B_{TM} = |(k_z c/\omega + Z^{(1)})(k_z c/\omega + Z^{(2)}) - (k_z c/\omega - Z^{(1)})(k_z c/\omega - Z^{(2)}) \exp(2ik_z a)|^2. \quad (84)$$

If we separate the PW and EW contributions to Eq. (82), it is easy to verify that Eqs. (78)–(80) are equivalent to Eqs. (82)–(84) in the impedance theory of heat transfer, provided that the reflection coefficients are taken to be those of impedance theory in Eq. (28).

8 Numerical results for heat transfer and emittivity

It should be noted that, according to Eq.(82), the value of S is very sensitive to the real part $\text{Re}Z(\omega)$ of the

impedance function, at angular frequencies ω of the order of $k_B T/\hbar$. It is also important to observe that at small separations a , S receives a large contribution from the EW. Since, as seen from Table 1, thermally exited EW are of great importance for the determination of the thermal correction $\Delta P(a, T)$ to the Casimir pressure, it is clear that a measurement of S would provide an independent verification of the validity of the impedance function, used in the evaluation of $\Delta P(a, T)$. We have estimated numerically the heat transfer S for three choices of the impedance functions, Z_D , Z_N and Z_t , that were discussed in Sec. 6. In Fig. 3, we show plots of the radiated power for two plates of Au as a function of the separation a for $T_1 = 320$ K and $T_2 = 300$ K. The three lines are for the standard Lifshitz theory with the Drude dielectric function in Eq. (33) (short-dashed line), for the impedance theory with the impedance Z_N of the normal-skin effect in Eq. (32) (long-dashed line), and again for the impedance theory, but this time with the impedance Z_D corresponding to the Drude model in Eq. (33) (dotted line). The band between the solid lines 1 and 2 is related to the impedance function Z_t in Eq. (75), with the upper and lower boundaries corresponding to $\beta = 0.08$ eV and $\beta = 0.125$ eV, respectively. The line for $Z = Z_p$ in Eq. (73) is not displayed, because it reproduces $\text{Re}Z_p$ inaccurately and the corresponding values for S are over two orders of magnitude smaller than those for, say, Z_t . Note that the dielectric permittivity approach with ε corresponding to Z_t leads to almost the same results as are presented by the band between the solid lines 1 and 2 in Fig. 3. The only difference is that at short separations the lines 1 and 2 are a bit shifted towards smaller values of S , while preserving the same asymptotic values at large separations. As we see, Lifshitz theory using the dielectric permittivity ε_D , as well as the impedance theory for $Z = Z_D$ and $Z = Z_N$, both lead to values for S that are several times larger than those implied by the impedance Z_t or respective dielectric permittivity, for separations around or less than half micrometer. To a large extent, these large differences are due to considerably different contributions from the TE EW in the various models. In Fig. 4, we show a plot of the relative contribution to S from TE EW, for the models considered in Fig. 3. As we see, the TE EW play an important role in the entire range of separations considered.

Besides heat transfer, another interesting quantity to consider is the total emittivity $e(T)$ of the metal, defined as:

$$e(T) = \frac{\Phi(T)}{\Phi_{\text{BB}}(T)}. \quad (85)$$

Here, $\Phi(T)$ is the total flux of radiation from a unit surface of a metal defined in Eq. (81), while $\Phi_{\text{BB}}(T)$ is the flux from a black body. According to Stefan law, the latter quantity is equal to

$$\Phi_{\text{BB}}(T) = \Theta T^4, \quad (86)$$

where $\Theta = 5.6704 \times 10^{-8} \text{ W m}^{-2} \text{ K}^{-4}$. For a polished surface of gold at $T = 295$ K, the tabulated value is $e \approx 0.02$.

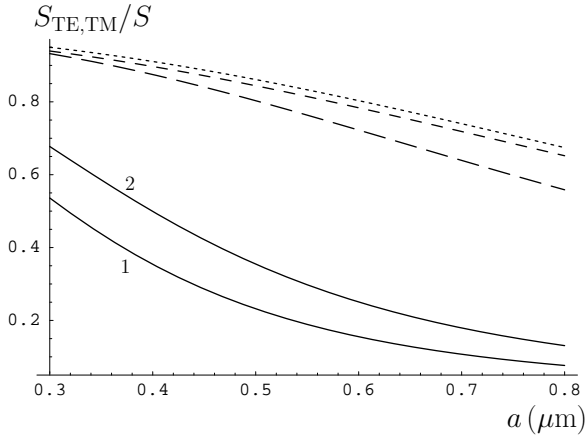


Fig. 4. Plots of the relative contributions of TE EW to the total radiative heat transfer between two Au plates at temperatures $T_1 = 320$ K and $T_2 = 300$ K as a function of separation. Lines are notated as in Fig. 3.

In Table 3 we report the calculated values for e , corresponding to the same models as considered in Fig. 3. The interval of values for e , appearing in the fifth column in the case of $Z = Z_t$, is related to the values of β considered in Fig. 3, with the lower and upper values of e corresponding to $\beta = 0.125$ eV and $\beta = 0.08$ eV, respectively. As is seen in Table III, the measured emittivity is better described by the impedance of the normal skin effect and by the generalized impedance of the infrared optics Z_t . However, any definite conclusion is impossible without information on the precision of emittivity measurements.

9 Conclusions and discussion

In the first part of this paper we have implemented the thermodynamic test for two different choices for the surface impedance of a metal, that are used in the theory of the thermal Casimir force. By making analytic perturbation expansions in powers of small parameters, we have obtained the asymptotic expressions for the free energy and entropy of a fluctuating field at low temperatures. This was done by using the Leontovich impedances of the infrared optics Z_i and of the Drude model Z_D . The Leontovich impedance of the infrared optics, extrapolated to low frequencies, withstood the thermodynamic test. The obtained asymptotic expressions for the free energy and entropy of a fluctuating field are found to be thermodynamically consistent. In particular, entropy becomes zero when temperature vanishes, i.e., the Nernst heat theorem is satisfied. On the other hand, the Leontovich impedance of the Drude model was shown to be thermodynamically inconsistent. In the case of metals with perfect crystal lattices the entropy at zero temperature was found to be positive and depending on the parameters of the system in violation of the Nernst heat theorem.

The above conclusions provoke two questions on how to correctly apply thermal quantum field theory in Mat-

subara formulation to real materials. Both the result of this paper and of [39,40] on the thermodynamic inconsistency of Z_D and ε_D , respectively, in the theory of the thermal Casimir force were obtained by using the idealization of perfect crystal lattice of a metal. In the presence of impurities there is a nonzero residual relaxation at $T = 0$, i.e., $\gamma(0) \neq 0$. As a result, at very low temperatures the first Matsubara frequencies may become less than $\gamma(0)$ and the entropy jumps steeply to zero. For metals with impurities, described by the dielectric permittivity of the Drude model, the vanishing of entropy at $T = 0$ was demonstrated in [41,42]. This, however, does not solve the problem arising for metals with perfect crystal lattices. Such metals have a nonzero relaxation $\gamma(T)$ at nonzero T and are commonly used as the basic model in the theory of electron-phonon interactions. For perfect crystal lattices with no impurities the Nernst heat theorem is proved in the framework of quantum statistical physics [72], and the violation of this theorem by the entropy of a fluctuating field is a problem of great concern. It is our opinion that the violation of the third law of thermodynamics by the Casimir entropy calculated using ε_D and Z_D warns about the inapplicability of the Drude model in the theory of the thermal Casimir force.

Another question to discuss is the physical meaning of the zero Matsubara frequency in the Lifshitz formula, Eq. (1), or of low frequencies in the equivalent form of it, Eq. (12), expressed in terms of real frequencies. Should the analytic expression for the impedance of a metal which is valid for frequencies around the characteristic frequency Ω_c , be extrapolated without modifications to quasistatic frequencies, as we did in Sec. 4, where we dealt with the impedance of infrared optics? Or, alternatively, should one use different impedance functions within different frequency regions in accordance with their applicability conditions? The latter approach was in fact used in Sec. 5 because the impedance of the Drude model coincides with the impedance of the infrared optics in the region of infrared frequencies around Ω_c and with the impedance of the normal skin effect in the region of quasistatic frequencies. Our results demonstrate that in spite of being rather natural to use different impedance functions in accordance with the frequency regions of their applicability, and not use any extrapolation, the actual situation is not so simple. As is shown in Sec. 4, the extrapolation of the impedance of infrared optics to zero Matsubara frequency satisfies the thermodynamic test, whereas the use of the Drude model impedance in Sec. 5, coinciding with the impedances of the normal skin effect and infrared optics in the appropriate frequency regions, violates thermodynamics. This should be compared with the results of [44,45,46,47,48] devoted to the Casimir interaction between two dielectrics and between metal and dielectric. In both cases the account of an actual dielectric response at quasistatic frequencies (i.e., the account of nonzero dc conductivity) results in contradiction with thermodynamics, whereas the extrapolation of the dielectric behavior at high frequencies to zero frequency satisfies the thermodynamic test. This leads us to argue that the response function of both a metal and a

dielectric to a real external electromagnetic field of very low, quasistatic, frequency is not related to the physical phenomenon of dispersion forces determined by the electromagnetic fluctuations of high frequencies. In terms of physical processes occurring at different frequencies the above discussed extrapolation would imply that in metal bodies the fluctuating electromagnetic field creates only pure imaginary currents related to the frequency region of infrared optics. However, if the characteristic frequency belongs to the region of infrared optics, real currents with typical frequencies of the normal skin effect cannot be created by the fluctuating field. The deeper understanding of these guesses may go beyond the scope of the Lifshitz theory.

In the second part of this paper we have performed a comparative phenomenological investigation of the thermal Casimir force between two parallel metal plates and of the radiative heat transfer which occurs between such plates when they are kept at different temperatures. Both phenomena are of the same physical nature because they are caused by electromagnetic fluctuations. As was discussed above, the problem of the thermal Casimir force meets with difficulties, and different controversial approaches to its resolution were proposed in the literature. These approaches are based on the use of various dielectric functions (the dielectric permittivities of the Drude and of the plasma model) or, alternatively, different forms of the Leontovich surface impedance. The selection between the approaches is done by the comparison of the obtained results with the requirements of thermodynamics and with the experimental data. In this paper we have demonstrated that the use of the impedance functions $Z_N(\omega)$ and $Z_D(\omega)$ (constructed using the dielectric permittivities of the normal skin effect and of the Drude model) to calculate the thermal correction to the Casimir force leads to contradiction with experiment at separations of a few hundred nanometers. Recall that earlier the use of the dielectric permittivity of the Drude model to calculate the thermal correction was also shown to be inconsistent with experiment. At the same time, both the dielectric permittivity of the plasma model and the corresponding impedances related to the region of infrared optics are consistent with experiment.

The radiative heat transfer between two plates was previously studied using the dielectric permittivity of the Drude model [32,60,61] and the related impedance $Z_D(\omega)$ [33]. These approaches, however, lead to a contradiction with experiment in the case of the thermal Casimir force. Because of this, it is of much interest to investigate the radiative heat transfer using the impedance of infrared optics. Lack of reliable experimental data for the power of heat transfer and resulting uncertainty with the experimental confirmation of the computations in [32,33,60,61] add importance to this aim.

Bearing in mind that the radiative heat transfer is very sensitive to the real part of the impedance function we have constructed the new impedance Z_t in the region of infrared optics. The real part of this impedance takes into account the tabulated optical data for the complex index

of refraction extrapolated to low frequencies in accordance with general theoretical requirements. The power of heat transfer calculated with this impedance is several times less than previous predictions at separations of a few hundred nanometers. These large differences are mainly explained by different contributions from the TE EW in the various models of a metal.

Both physical phenomena of the thermal Casimir force and of the radiative heat transfer are finding prospective applications in nanotechnology. This makes urgent to carry out new precise experiments in order to find what characterization of real metals is most adequate for the description of electromagnetic fluctuations.

Acknowledgements. V.B.B. and C.R. were partially supported by CNPq (Brazil) and by FAPESQ-Pb/CNPq (PRONEX). G.B. was partially supported by the PRIN SINTESI. G.L.K. and V.M.M. were supported by the University of Naples Federico II, under the program "Programma Internazionale di Modilità Docenti e Studenti", and by the PRIN SINTESI. They were also partially supported by CNPq, PRONEX and by Deutsche Forschungsgemeinschaft grants 436 RUS 113/789/0-2 and 0-3.

References

1. E. M. Lifshitz, Zh. Eksp. Teor. Fiz. **29**, 94 (1956) [Sov. Phys. JETP **2**, 73 (1956)].
2. I. E. Dzyaloshinskii, E. M. Lifshitz, L. P. Pitaevskii, Usp. Fiz. Nauk **73**, 381 (1961) [Sov. Phys. Usp. (USA) **4**, 153 (1961)].
3. E. M. Lifshitz, L. P. Pitaevskii, *Statistical Physics*, Part 2 (Pergamon Press, Oxford, 1980).
4. K. Schram, Phys. Lett. A **43**, 283 (1973).
5. P. W. Milonni, *The Quantum Vacuum* (Academic Press, San Diego, 1994).
6. F. Zhou, L. Spruch, Phys. Rev. A **52**, 297 (1995).
7. C. Genet, A. Lambrecht, S. Reynaud, Phys. Rev. A **67**, 043811 (2003).
8. M. Bordag, U. Mohideen, V. M. Mostepanenko, Phys. Rep. **353**, 1 (2001).
9. S. K. Lamoreaux, Phys. Rev. Lett. **78**, 5 (1997).
10. U. Mohideen, A. Roy, Phys. Rev. Lett. **81**, 4549 (1998); G. L. Klimchitskaya, A. Roy, U. Mohideen, V. M. Mostepanenko, Phys. Rev. A **60**, 3487 (1999).
11. A. Roy, C.-Y. Lin, U. Mohideen, Phys. Rev. D **60**, 111101(R) (1999).
12. B. W. Harris, F. Chen, U. Mohideen, Phys. Rev. A **62**, 052109 (2000); F. Chen, G. L. Klimchitskaya, U. Mohideen, V. M. Mostepanenko, Phys. Rev. A **69**, 022117 (2004).
13. T. Ederth, Phys. Rev. A **62**, 062104 (2000).
14. F. Chen, U. Mohideen, G. L. Klimchitskaya, V. M. Mostepanenko, Phys. Rev. Lett. **88**, 101801 (2002); Phys. Rev. A **66**, 032113 (2002).
15. G. Bressi, G. Carugno, R. Onofrio, G. Ruoso, Phys. Rev. Lett. **88**, 041804 (2002).
16. R. S. Decca, E. Fischbach, G. L. Klimchitskaya, D. E. Krause, D. López, V. M. Mostepanenko, Phys. Rev. D **68**, 116003 (2003).

17. R. S. Decca, D. López, E. Fischbach, G. L. Klimchitskaya, D. E. Krause, V. M. Mostepanenko, *Ann Phys. (N.Y.)* **318**, 37 (2005).
18. G. L. Klimchitskaya, R. S. Decca, E. Fischbach, D. E. Krause, D. López, V. M. Mostepanenko, *Int. J. Mod. Phys. A* **20**, 2205 (2005).
19. R. S. Decca, D. López, E. Fischbach, G. L. Klimchitskaya, D. E. Krause, V. M. Mostepanenko, *Phys. Rev. D* **75**, 077101, (2007).
20. R. S. Decca, D. López, E. Fischbach, G. L. Klimchitskaya, D. E. Krause, V. M. Mostepanenko, *Eur. Phys. J. C* (2007), to appear, DOI 10.1140/epjc/s10052-007-0346-z.
21. F. Chen, U. Mohideen, G. L. Klimchitskaya, V. M. Mostepanenko, *Phys. Rev. A* **72**, 020101(R) (2005).
22. F. Chen, U. Mohideen, G. L. Klimchitskaya, V. M. Mostepanenko, *Phys. Rev. A* **74**, 022103 (2006).
23. F. Chen, G. L. Klimchitskaya, V. M. Mostepanenko, U. Mohideen, *Phys. Rev. Lett.* **97**, 170402 (2006).
24. F. Chen, G. L. Klimchitskaya, V. M. Mostepanenko, U. Mohideen, *Optics Express* **15**, 4823 (2007).
25. H. B. Chan, V. A. Aksyuk, R. N. Kleiman, D. J. Bishop, F. Capasso, *Science* **291**, 1941 (2001); *Phys. Rev. Lett.* **87**, 211801 (2001).
26. E. Buks, M. L. Roukes, *Phys. Rev. B* **63**, 033402 (2001).
27. E. V. Blagov, G. L. Klimchitskaya, V. M. Mostepanenko, *Phys. Rev. B* **71**, 235401 (2005); G. L. Klimchitskaya, E. V. Blagov, V. M. Mostepanenko, *J. Phys. A: Math. Gen.* **39**, 6481 (2006).
28. M. Bordag, B. Geyer, G. L. Klimchitskaya, V. M. Mostepanenko, *Phys. Rev. B* **74**, 205431 (2006).
29. E. V. Blagov, G. L. Klimchitskaya, V. M. Mostepanenko, *Phys. Rev. B* **75**, 235413 (2007).
30. J. F. Babb, G. L. Klimchitskaya, V. M. Mostepanenko, *Phys. Rev. A* **70**, 042901 (2004).
31. M. Antezza, L. P. Pitaevskii, S. Stringari, *Phys. Rev. A* **70**, 053619 (2004).
32. A. I. Volokitin, B. N. J. Persson, *Phys. Rev. B* **63**, 205404 (2001); **69**, 045417 (2004).
33. G. Bimonte, *Phys. Rev. Lett.* **96**, 160401 (2006).
34. C. Genet, A. Lambrecht, S. Reynaud, *Phys. Rev. A* **62**, 012110 (2000).
35. M. Bordag, B. Geyer, G. L. Klimchitskaya, V. M. Mostepanenko, *Phys. Rev. Lett.* **85**, 503 (2000).
36. L. S. Brown, G. J. Maclay, *Phys. Rev.* **184**, 1272 (1969).
37. M. Boström, B. E. Sernelius, *Phys. Rev. Lett.* **84**, 4757 (2000).
38. J. S. Høye, I. Brevik, J. B. Aarseth, K. A. Milton, *Phys. Rev. E* **67**, 056116 (2003).
39. V. B. Bezerra, G. L. Klimchitskaya, V. M. Mostepanenko, *Phys. Rev. A* **65**, 052113 (2002); **66**, 062112 (2002).
40. V. B. Bezerra, G. L. Klimchitskaya, V. M. Mostepanenko, C. Romero, *Phys. Rev. A* **69**, 022119 (2004).
41. M. Boström, B. E. Sernelius, *Physica A* **339**, 53 (2004).
42. I. Brevik, J. B. Aarseth, J. S. Høye, K. A. Milton, *Phys. Rev. E* **71**, 056101 (2005).
43. G. L. Klimchitskaya, U. Mohideen, V. M. Mostepanenko, *J. Phys. A: Math. Theor.* **40**, 339(F) (2007).
44. B. Geyer, G. L. Klimchitskaya, V. M. Mostepanenko, *Phys. Rev. D* **72**, 085009 (2005).
45. G. L. Klimchitskaya, B. Geyer, V. M. Mostepanenko, *J. Phys. A: Math. Gen.* **39**, 6495 (2006).
46. B. Geyer, G. L. Klimchitskaya, V. M. Mostepanenko, *Phys. Rev. A* **72**, 022111 (2005).
47. B. Geyer, G. L. Klimchitskaya, V. M. Mostepanenko, *Int. J. Mod. Phys. A* **21**, 5007 (2006).
48. B. Geyer, G. L. Klimchitskaya, V. M. Mostepanenko, *Ann. Phys. (N.Y.)* (2007), to appear, DOI 10.1016/j.aop.2007.04.005.
49. J. S. Høye, I. Brevik, J. B. Aarseth, K. A. Milton, *J. Phys. A: Math. Gen.* **39**, 6031 (2006).
50. V. M. Mostepanenko, V. B. Bezerra, R. S. Decca, E. Fischbach, B. Geyer, G. L. Klimchitskaya, D. E. Krause, D. López, C. Romero, *J. Phys. A: Math. Gen.* **39**, 6589 (2006).
51. L. D. Landau, E. M. Lifshitz, L. P. Pitaevskii, *Electrodynamics of Continuous Media* (Pergamon Press, Oxford, 1984).
52. E. I. Kats, *Zh. Eksp. Teor. Fiz.* **73**, 212 (1977) [*Sov. Phys. JETP* **46**, 109 (1977)].
53. V. B. Bezerra, G. L. Klimchitskaya, C. Romero, *Phys. Rev. A* **65**, 012111 (2002).
54. B. Geyer, G. L. Klimchitskaya, V. M. Mostepanenko, *Phys. Rev. A* **67**, 062102 (2003).
55. V. B. Svetovoy, M. V. Lokhanin, *Phys. Rev. A* **67**, 022113 (2003).
56. B. Geyer, G. L. Klimchitskaya, V. M. Mostepanenko, *Phys. Rev. A* **70**, 016102 (2004).
57. J. R. Torgerson, S. K. Lamoreaux, *Phys. Rev. E* **70**, 047102 (2004).
58. G. Bimonte, *Phys. Rev. E* **73**, 048101 (2006).
59. J. R. Torgerson, S. K. Lamoreaux, *Phys. Rev. E* **73**, 048102 (2006).
60. D. Polder, M. Van Hove, *Phys. Rev. B* **4**, 3303 (1971).
61. J. J. Loomis, H. J. Maris, *Phys. Rev. B* **50**, 18517 (1994).
62. V. M. Mostepanenko, N. N. Trunov, *The Casimir Effect and its Applications* (Clarendon Press, Oxford, 1997).
63. T. Emig, R. Büscher, *Nucl. Phys. B* **696**, 468 (2004).
64. E. M. Lifshitz, L. P. Pitaevskii, *Physical Kinetics* (Pergamon Press, Oxford, 1981).
65. G. L. Klimchitskaya, V. M. Mostepanenko, *Phys. Rev. B* **75**, 036101 (2007).
66. V. B. Bezerra, R. S. Decca, E. Fischbach, B. Geyer, G. L. Klimchitskaya, D. E. Krause, D. López, V. M. Mostepanenko, C. Romero, *Phys. Rev. E* **73**, 028101 (2006).
67. I. Brevik, J. B. Aarseth, *J. Phys. A: Math. Gen.* **39**, 6187 (2006).
68. N. W. Ashcroft, N. D. Mermin, *Solid State Physics* (Saunders College Publishing, Philadelphia, 1976).
69. I. S. Gradshteyn, I. M. Ryzhik, *Table of Integrals, Series, and Products* (Academic Press, New York, 1994).
70. B. Geyer, G. L. Klimchitskaya, V. M. Mostepanenko, *Int. J. Mod. Phys. A* **16**, 3291 (2001).
71. C. Kittel, *Introduction to Solid State Physics* (Wiley, New York, 1996).
72. L. D. Landau, E. M. Lifshitz, *Statistical Physics, Part 1* (Pergamon, Oxford, 1980).
73. J. Feinberg, A. Mann, M. Revzen, *Ann. Phys. (N.Y.)* **288**, 103 (2001).
74. A. Scardicchio, R. L. Jaffe, *Nucl. Phys. B* **743**, 249 (2006).
75. *Handbook of Optical Constants of Solids*, ed. E. D. Palik (Academic, New York, 1985).
76. A. Lambrecht, S. Reynaud, *Eur. Phys. J. D* **8**, 309 (2000).
77. G. L. Klimchitskaya, U. Mohideen, V. M. Mostepanenko, *Phys. Rev. A* **61**, 062107 (2000).

78. M. Boström, B. E. Sernelius, Phys. Rev. A **61**, 046101 (2000).
79. S. M. Rytov, *Theory of Electric Fluctuations and Thermal Radiation* (Air Force Cambridge Research Center, Bedford, Mass., 1959); M. A. Leontovich, S. M. Rytov, Zh. Eksperim. i Teor. Fiz. **23**, 246 (1952).
80. C. M. Hargreaves, Phys. Lett. A **30**, 491 (1969).

Table 1. Thermal correction to the pressure between Au plates at $T = 300$ K (column 2) and different contributions to it as a function of separation computed using the impedance of the normal skin effect Z_N . See text for further discussion.

a (μm)	ΔP (mPa)	$\frac{\Delta P}{\Delta P^{\text{TM}}}$	$\frac{\Delta P_{\text{TE,EW}}}{\Delta P}$	$\frac{\Delta P_{\text{TE,PW}}}{\Delta P}$	$\frac{\Delta P_{\text{TM,EW}}}{\Delta P}$	$\frac{\Delta P_{\text{TM,PW}}}{\Delta P}$
0.2	-12.1	5.9×10^3	0.998	-9×10^{-5}	2×10^{-3}	-2×10^{-4}
0.25	-5.4	2.6×10^3	0.997	-7×10^{-5}	3.6×10^{-3}	-2×10^{-4}
0.3	-2.8	1.4×10^3	0.995	-3×10^{-6}	5×10^{-3}	-3×10^{-4}
0.35	-1.6	7.8×10^2	0.994	1.5×10^{-4}	6×10^{-3}	-3×10^{-4}
0.4	-0.96	4.7×10^2	0.992	5×10^{-4}	8×10^{-3}	-2×10^{-4}
1	-0.032	16	0.91	0.03	0.03	0.02

Table 2. Thermal correction to the pressure between Au plates at $T = 300$ K (column 2) and different contributions to it as a function of separation computed using the impedance of infrared optics Z_p . See text for further discussion.

a (μm)	ΔP (mPa)	$\frac{\Delta P}{\Delta P^{\text{TM}}}$	$\frac{\Delta P_{\text{TE,EW}}}{\Delta P}$	$\frac{\Delta P_{\text{TE,PW}}}{\Delta P}$	$\frac{\Delta P_{\text{TM,EW}}}{\Delta P}$	$\frac{\Delta P_{\text{TM,PW}}}{\Delta P}$
0.2	-0.0097	4.7	-0.76	0.10	1.55	0.1
0.25	-0.0081	4.0	-0.43	0.13	1.18	0.12
0.3	-0.0070	3.4	-0.26	0.14	0.97	0.14
0.35	-0.0059	2.9	-0.18	0.17	0.84	0.17
0.4	-0.0051	2.5	-0.13	0.20	0.73	0.20
1	-0.0026	1.3	-0.01	0.39	0.2	0.4

Table 3. Values of the emittivity e of Au at $T = 295$ K.

Measured	Lifshitz ($\varepsilon = \varepsilon_D$)	$Z = Z_N$	$Z = Z_D$	$Z = Z_t$	$Z = Z_p$
0.02	0.0098	0.023	0.0098	0.013÷0.016	2.5×10^{-4}